American Journal of Physics and Applications
2016; 4(2): 27-49
http://www.sciencepublishinggroup.com/j/ajpa
doi: 10.11648/j.ajpa.20160402.12
ISSN: 2330-4286 (Print); ISSN: 2330-4308 (Online)

Review Article

Recent Developments in the X-ray Reflectivity Analysis

Yoshikazu Fujii

Center for Supports to Research and Education Activities, Kobe University, Nada, Kobe, Japan

Email address:
fujiiyos@kobe-u.ac.jp

To cite this article:
Yoshikazu Fujii. Recent Developments in the X-ray Reflectivity Analysis. *American Journal of Physics and Applications.* Vol. 4, No. 2, 2016, pp. 27-49. doi: 10.11648/j.ajpa.20160402.12

Received: February 8, 2016; **Accepted**: February 16, 2016; **Published**: March 17, 2016

Abstract: X-ray reflectivity (XRR) is a powerfull tool for investigations on surface and interface structures of multilayered thin film materials. In the conventional XRR analysis, the X-ray reflectivity has been calculated based on the Parratt formalism, accounting for the effect of roughness by the theory of Nevot-Croce conventionally. However, the calculated results have shown often strange behaviour where interference effects would increase at a rough surface. The strange result had its origin in a serious mistake that the diffuse scattering at the rough interface was not taken into account in the equation. Then we developed new improved formalism to correct this mistake. However, the estimated surface and interface roughnesses from the x-ray reflectivity measurements did not correspond to the TEM image observation results. For deriving more accurate formalism of XRR, we tried to compare the measurements of the surface roughness of the same sample by atomic force microscopy (AFM), high-resolution Rutherford backscattering spectroscopy (HRBS) and XRR. The results of analysis showed that the effective roughness measured by XRR might depend on the angle of incidence. Then we introduced the effective roughness with depending on the incidence angle of X-ray. The new improved XRR formalism derived more accurate surface and interface roughness with depending on the size of coherent X-rays probing area, and derived the roughness correlation function and the lateral correlation length. In this review, an improved XRR formalism, considering the diffuse scattering and the effective roughness, is presented. The formalism derives an accurate analysis of the x-ray reflectivity from a multilayer surface of thin film materials.

Keywords: X-ray Reflectivity, Surface and Interface Roughness, Multilayered Thin Film, Buried Interface

1. Introduction

X-ray scattering spectroscopy is a powerful tool for investigations on rough surface and interface structures of multilayered thin film materials, [1-41] and X-ray reflectometry is used for such investigations of various materials in many fields. [15, 16, 20-41] In many previous studies in X-ray reflectometry, the X-ray reflectivity was calculated based on the Parratt formalism, [1] coupled with the use of the theory of Nevot and Croce to include roughness. [2] However, the calculated results of the X-ray reflectivity done in this way often showed strange results where the amplitude of the oscillation due to the interference effects would increase for a rougher surface.

Because the x-ray scattering vector in a specular reflectivity measurement is normal to the surface, it provides the density profile solely in the direction perpendicular to surface. Specular reflectivity measurements can yield the magnitude of the average roughness perpendicular to surface and interfaces, but cannot give information about the lateral extent of the roughness. In previous studies, the effect of roughness on the calculation of the x-ray reflectivity only took into account the effect of the density changes of the medium in a direction normal to the surface and interface. On the other hand, diffuse scattering can provide information about the lateral extent of the roughness. In contrast to previous calculations of the x-ray reflectivity, in the present analysis we consider the effect of a decrease in the intensity of penetrated x-rays due to diffuse scattering at a rough surface and rough interface.

In this review, we show that the strange result has its origin in a currently used equation due to a serious mistake in which the Fresnel transmission coefficient in the reflectivity equation is increased at a rough interface, and the increase in the transmission coefficient completely overpowers any decrease in the value of the reflection coefficient because of a lack of consideration of diffuse scattering. The mistake in Nevot and

Croce's treatment originates in the fact that the modified Fresnel coefficients were calculated based on the theory which contains the x-ray energy conservation rule at surface and interface. In their discussion, the transmission coefficients were replaced approximately by the reflection coefficients by the ignoring diffuse scattering term at the rough interface, and according to the principle of conservation energy at the rough interface also. The errors of transmittance without the modification cannot be ignored. It is meaningless to try to precisely match the numerical result based on a wrong calculating formula even to details of the reflectivity profile of the experimental result. Thus, because Nevot and Croce's treatment of the Parratt formalism contains a fundamental mistake regardless of the size of roughness, this approach needs to be corrected. Then we developed new improved formalism to correct this mistake. The calculated reflectivity obtained by the use of this accurate reflectivity equation gives a physically reasonable result, and should enable the structure of buried interfaces to be analyzed more accurately. However, the estimated surface and interface roughnesses from the x-ray reflectivity measurements did not correspond to the TEM image observation results. Then for deriving more accurate formalism of XRR, we tried to compare the measurements of the surface roughness of the same sample by atomic force microscopy (AFM), high-resolution Rutherford backscattering spectroscopy (HRBS) and XRR. The results of analysis showed that the effective roughness measured by XRR might depend on the angle of incidence. Then we introduced the effective roughness with depending on the incidence angle of X-ray. The new improved XRR formalism derived more accurate surface and interface roughness with depending on the size of coherent X-rays probing area, and derived the roughness correlation function and the lateral correlation length. In this review, an improved XRR formalism, considering the diffuse scattering and the effective roughness, is presented. The formalism derives an accurate analysis of the x-ray reflectivity from a multilayer surface of thin film materials. This article is the review article that summarized the research articles [33-41] and the later study.

2. X-ray Reflectivity Analysis

In the first subsection, we consider the calculation of the x-ray reflectivity from a multilayer material by the Parratt formalism, [1] and in the next subsection, the calculation of the x-ray reflectivity when roughness exists in the surface and the interface is considered.

2.1. X-ray Reflectivity from a Multilayer Material with a Flat Surface and Flat Interface

The intensity of x-rays propagating in the surface layers of a material, *i.e.*, the electric and magnetic fields, can be obtained from Maxwell's equations. [19] The effects of the material on the x-ray intensity are characterized by a complex refractive index n, which varies with depth. We divide a material in which the density changes continuously with depth into N layers with an index j. The complex refractive index of the j-th layer is n_j. The vacuum is denoted as $j = 0$ and $n_0 = 1$. The thickness of the j-th layer is h_j, the thickness of the bottom layer being assumed to be infinite.

The reflectance of an N-layer multilayer system can be calculated using the recursive formalism given by Parratt. [1] In the following, we show in detail the process of obtaining Parratt's expression and, further, show that this expression requires conservation of energy at the interface. We go on to show that the dispersion of the energy by interface roughness cannot be correctly accounted for Parratt's expression.

Following that approach, let n_j be the refractive index of the j-th layer, defined as

$$n_j = 1 - \delta_j - \mathrm{i}\beta_j, \tag{1}$$

where δ_j and β_j are the real and imaginary parts of the refractive index. These optical constants are related to the atomic scattering factor and electron density of the j-th layer material.

For x-rays of wavelength λ, the optical constants of the j-th layer material consisting of N_{ij} atoms per unit volume can be expressed as

$$\delta_j = \frac{\lambda^2 \mathrm{r}_e}{2\pi}\sum_i f_{1i}N_{ij}\ ,\quad \beta_j = \frac{\lambda^2 \mathrm{r}_e}{2\pi}\sum_i f_{2i}N_{ij}\ , \tag{2}$$

where r_e is the classical electron radius and f_{1i} and f_{2i} are the real and imaginary parts of the atomic scattering factor of the i-th element atom, respectively.

We take the vertical direction to the surface as the z axis, with the positive direction pointing towards the bulk. The scattering plane is made the x-z plane. The wave vector $\boldsymbol{k}_j$ of the j-th layer is related to the refractive index n_j of the j-th layer by

$$\frac{\boldsymbol{k}_j \cdot \boldsymbol{k}_j}{n_j^2} = \frac{\omega^2}{c^2} = const\,, \tag{3}$$

and, as this necessitates that the x, y-direction components of the wave vector are constant, then the z-direction component of the wave vector of the j-th layer is

$$k_{j,z} = \sqrt{n_j^2 \boldsymbol{k}_0 \cdot \boldsymbol{k}_0 - k_{0,x}^2}\ . \tag{4}$$

In the 0-th layer, *i.e.*, in vacuum,

$$n_0 = 1,\ \ \boldsymbol{k}_0 \cdot \boldsymbol{k}_0 = k^2,\ \ k = \frac{2\pi}{\lambda} = \frac{\omega}{c}\,. \tag{5}$$

In the j-th layer, the components of the wave vector are

$$k_{j,\mathrm{x}} = k\cos\theta,\ \ k_{j,y} = 0,\ \ k_{j,z} = k\sqrt{n_j^2 - \cos^2\theta} \tag{6}$$

The electric field of x-ray radiation at a glancing angle of incidence θ is expressed as

$$\boldsymbol{E}_0(z) = \boldsymbol{A}_0 \exp[i(\boldsymbol{k}_0 \cdot \boldsymbol{r} - \omega t)]\,. \tag{7}$$

The incident radiation is usually decomposed into two

geometries to simplify the analysis, one with the incident electric field E parallel to the plane of incidence (p-polarization) and one with E perpendicular to that plane (s-polarization). An arbitrary incident wave can be represented in terms of these two polarizations. Thus, E_{0x} and E_{0z} correspond to p-polarization, and E_{0y} to s-polarization; those components of the amplitude's electric vector are expressed as

$$A_{0x} = -A_{0p}\sin\theta\,,\quad A_{0y} = A_{0s}\,,\quad A_{0z} = A_{0p}\cos\theta \tag{8}$$

The components of the wave vector of the incident x-rays are

$$k_{0x} = k\cos\theta\,,\quad k_{0y} = 0\,,\quad k_{0z} = k\sin\theta \tag{9}$$

The electric field of reflected x-ray radiation of exit angle θ is expressed as

$$\boldsymbol{E}'_0(z) = \boldsymbol{A}'_0\exp[i(\boldsymbol{k}'_0\cdot\boldsymbol{r} - \omega t)]. \tag{10}$$

where

$$k'_{0x} = k_{0x}\,,\quad k'_{0y} = 0\,,\quad k'_{0z} = -k_{0z}\,. \tag{11}$$

Because an x-ray is a transverse wave, the amplitude and the wave vector are orthogonal as follows,

$$\boldsymbol{A}_j\cdot\boldsymbol{k}_j = 0\quad,\quad \boldsymbol{A}'_j\cdot\boldsymbol{k}'_j = 0\,. \tag{12}$$

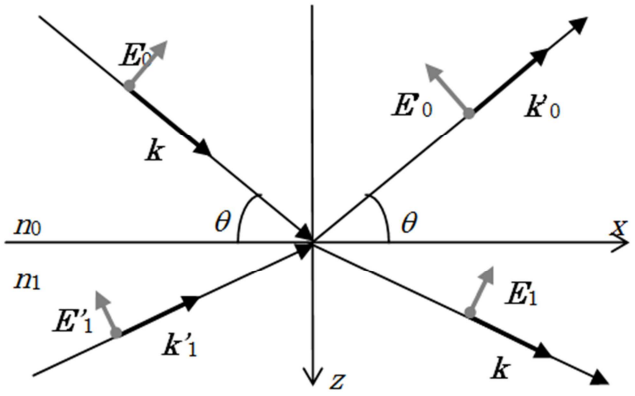

Figure 1. *Reflected and transmitted x-rays.*

We consider the relation of the electric field $\boldsymbol{E}_0$ of x-rays incident at a flat surface from vacuum, the electric field $\boldsymbol{E}_1$ of x-rays propagating in the first layer material, the electric field $\boldsymbol{E'}_0$ of x-rays reflected from the surface exit to vacuum, and the electric field $\boldsymbol{E'}_1$ of x-rays propagating toward to the surface in the first layer material, as shown in Figure 1.

The electric fields $\boldsymbol{E}_1$, $\boldsymbol{E'}_1$ in the first layer material below the surface are expressed as

$$\boldsymbol{E}_1(z) = \boldsymbol{A}_1\exp[i(\boldsymbol{k}_1\cdot\boldsymbol{r} - \omega t)]$$

$$\boldsymbol{E}'_1(z) = \boldsymbol{A}'_1\exp[i(\boldsymbol{k}'_1\cdot\boldsymbol{r} - \omega t)], \tag{13}$$

where

$$k'_{1x} = k_{1x}\,,\quad k'_{1y} = 0\,,\quad k'_{1z} = -k_{1z}\,, \tag{14}$$

$$k_{1,\mathrm{x}} = k\cos\theta\,,\quad k_{1y} = 0\,,\quad k_{1,z} = k\sqrt{n_1^{2} - \cos^2\theta}\,. \tag{15}$$

The relation of the amplitudes A_0, A'_0, A_1, and A'_1 can be found from the continuity equations of the electric fields for the interface between the 0-th and 1-th layers as follows

$$A_{0,x} + A'_{0,x} = A_{1,x} + A'_{1,x}\,,\quad A_{0,y} + A'_{0,y} = A_{1,y} + A'_{1,y}\,, \tag{16}$$

$$k_{0,x}A_{0,x} + k'_{0,x}A'_{0,x} = k_{1,x}A_{1,x} + k'_{1,x}A'_{1,x}\,, \tag{17}$$

$$k_{0,y}A_{0,y} + k'_{0,y}A'_{0,y} = k_{1,y}A_{1,y} + k'_{1,y}A'_{1,y}\,, \tag{18}$$

Another relation of the amplitudes A_0, A'_0, A_1, and A'_1 can be found from the continuity equations of the magnetic fields for the interface between the 0-th and 1-th layers are shown below

$$\begin{aligned} &k_{0,z}A_{0,y} - k_{0,y}A_{0,z} + k'_{0,z}A'_{0,y} - k'_{0,y}A'_{0,z} \\ &= k_{1,z}A_{1,y} - k_{1,y}A_{1,z} + k'_{1,z}A'_{1,y} - k'_{1,y}A'_{1,z}\end{aligned}\,, \tag{19}$$

$$\begin{aligned} &k_{0,z}A_{0,x} - k_{0,x}A_{0,z} + k'_{0,z}A'_{0,x} - k'_{0,x}A'_{0,z} \\ &= k_{1,z}A_{1,x} - k_{1,x}A_{1,z} + k'_{1,z}A'_{1,x} - k'_{1,x}A'_{1,z}\end{aligned}\,, \tag{20}$$

From the above equations, these amplitudes are related by the Fresnel coefficient tensor $\boldsymbol{\Phi}$ for refraction and the Fresnel coefficient tensor $\boldsymbol{\Psi}$ for reflection as follows

$$\begin{pmatrix}\boldsymbol{A}'_0\\ \boldsymbol{A}_1\end{pmatrix} = \begin{pmatrix}\boldsymbol{\Psi}_{0,1} & \boldsymbol{\Phi}_{1,0}\\ \boldsymbol{\Phi}_{0,1} & \boldsymbol{\Psi}_{1,0}\end{pmatrix}\begin{pmatrix}\boldsymbol{A}_0\\ \boldsymbol{A}'_1\end{pmatrix}. \tag{21}$$

Here, the Fresnel coefficient tensor $\boldsymbol{\Phi}$ for refraction at the interface between the 0-th and 1-th layers is given by

$$\begin{aligned}
&\Phi_{0,1,xx} = \frac{2k_{1,z}\boldsymbol{k}_0\cdot\boldsymbol{k}_0}{k_{0,z}\boldsymbol{k}_1\cdot\boldsymbol{k}_1 + k_{1,z}\boldsymbol{k}_0\cdot\boldsymbol{k}_0} && \Phi_{1,0,xx} = \frac{2k_{0,z}\boldsymbol{k}_1\cdot\boldsymbol{k}_1}{k_{0,z}\boldsymbol{k}_1\cdot\boldsymbol{k}_1 + k_{1,z}\boldsymbol{k}_0\cdot\boldsymbol{k}_0}\\
&\Phi_{0,1,yy} = \frac{2k_{0,z}}{k_{0,z} + k_{1,z}} && \Phi_{1,0,yy} = \frac{2k_{1,z}}{k_{1,z} + k_{0,z}}\\
&\Phi_{0,1,zz} = \frac{2k_{0,z}\boldsymbol{k}_0\cdot\boldsymbol{k}_0}{k_{0,z}\boldsymbol{k}_1\cdot\boldsymbol{k}_1 + k_{1,z}\boldsymbol{k}_0\cdot\boldsymbol{k}_0}\,, && \Phi_{1,0,zz} = \frac{2k_{1,z}\boldsymbol{k}_1\cdot\boldsymbol{k}_1}{k_{0,z}\boldsymbol{k}_1\cdot\boldsymbol{k}_1 + k_{1,z}\boldsymbol{k}_0\cdot\boldsymbol{k}_0}\\
&\Phi_{0,1,xy} = \Phi_{0,1,yx} = \Phi_{0,1,yz} = 0 && \Phi_{1,0,xy} = \Phi_{1,0,yx} = \Phi_{1,0,yz} = 0\\
&\Phi_{0,1,zy} = \Phi_{0,1,zx} = \Phi_{0,1,xz} = 0 && \Phi_{1,0,zy} = \Phi_{1,0,zx} = \Phi_{1,0,xz} = 0
\end{aligned} \tag{22}$$

The Fresnel coefficient tensor $\boldsymbol{\Psi}$ for reflection from the interface between the 0-th and 1-th layers is given by

$$\begin{aligned}
&\Psi_{0,1,xx} = \frac{k_{1,z}\boldsymbol{k}_0\cdot\boldsymbol{k}_0 - k_{0,z}\boldsymbol{k}_1\cdot\boldsymbol{k}_1}{k_{0,z}\boldsymbol{k}_1\cdot\boldsymbol{k}_1 + k_{1,z}\boldsymbol{k}_0\cdot\boldsymbol{k}_0} && \Psi_{1,0,xx} = \frac{k_{0,z}\boldsymbol{k}_1\cdot\boldsymbol{k}_1 - k_{1,z}\boldsymbol{k}_0\cdot\boldsymbol{k}_0}{k_{0,z}\boldsymbol{k}_1\cdot\boldsymbol{k}_1 + k_{1,z}\boldsymbol{k}_0\cdot\boldsymbol{k}_0}\\
&\Psi_{0,1,yy} = \frac{k_{0,z} - k_{1,z}}{k_{0,z} + k_{1,z}} && \Psi_{1,0,yy} = \frac{k_{1,z} - k_{0,z}}{k_{0,z} + k_{1,z}}\\
&\Psi_{0,1,zz} = -\frac{k_{1,z}\boldsymbol{k}_0\cdot\boldsymbol{k}_0 - k_{0,z}\boldsymbol{k}_1\cdot\boldsymbol{k}_1}{k_{0,z}\boldsymbol{k}_1\cdot\boldsymbol{k}_1 + k_{1,z}\boldsymbol{k}_0\cdot\boldsymbol{k}_0}\,, && \Psi_{1,0,zz} = \frac{k_{1,z}\boldsymbol{k}_0\cdot\boldsymbol{k}_0 - k_{0,z}\boldsymbol{k}_1\cdot\boldsymbol{k}_1}{k_{0,z}\boldsymbol{k}_1\cdot\boldsymbol{k}_1 + k_{1,z}\boldsymbol{k}_0\cdot\boldsymbol{k}_0}\\
&\Psi_{0,1,xy} = \Psi_{0,1,yx} = \Psi_{0,1,yz} = 0 && \Psi_{1,0,xy} = \Psi_{1,0,yx} = \Psi_{1,0,yz} = 0\\
&\Psi_{0,1,zy} = \Psi_{0,1,zx} = \Psi_{0,1,xz} = 0 && \Psi_{1,0,zy} = \Psi_{1,0,zx} = \Psi_{1,0,xz} = 0
\end{aligned} \tag{23}$$

Here, we consider the reflection from a flat surface of a single layer. The reflection coefficient is defined as the ratio $R_{0,1}$ of the reflected electric field to the incident electric field at the surface of the material. The reflection coefficient $R_{0,1}$ from a single-layer flat surface is equal to the Fresnel coefficient Ψ_{01} for reflection, as the following shows

$$\boldsymbol{A'}_0 = \boldsymbol{R}_{0,1}\boldsymbol{A}_0 = \boldsymbol{\Psi}_{0,1}\boldsymbol{A}_0 \tag{24}$$

In general, when x-rays that are linearly polarized at an angle χ impinge on the surface at an angle of incidence θ, the components of the amplitude's electric vector are expressed as

$$\boldsymbol{A}_0 = \begin{pmatrix} A_{0x} \\ A_{0y} \\ A_{0z} \end{pmatrix} = \begin{pmatrix} -A_{0p}\sin\theta \\ A_{0s} \\ A_{0p}\cos\theta \end{pmatrix}, \quad \begin{pmatrix} A_{0p} \\ A_{0s} \end{pmatrix} = \begin{pmatrix} A_0\sin\chi \\ A_0\cos\chi \end{pmatrix} \tag{25}$$

the amplitudes of reflected x-ray radiation are expressed as

$$\boldsymbol{A'}_0 = \begin{pmatrix} A'_{0x} \\ A'_{0y} \\ A'_{0z} \end{pmatrix} = \begin{pmatrix} \Psi_{0,1,xx} & 0 & 0 \\ 0 & \Psi_{0,1,yy} & 0 \\ 0 & 0 & \Psi_{0,1,zz} \end{pmatrix} \begin{pmatrix} A_{0x} \\ A_{0y} \\ A_{0z} \end{pmatrix}. \tag{26}$$

$$\boldsymbol{A'}_0 = \begin{pmatrix} A'_{0x} \\ A'_{0y} \\ A'_{0z} \end{pmatrix} = A_0 \begin{pmatrix} -\Psi_{0,1,xx}\sin\chi\sin\theta \\ \Psi_{0,1,yy}\cos\chi \\ \Psi_{0,1,zz}\sin\chi\cos\theta \end{pmatrix}. \tag{27}$$

The x-ray reflectivity R is,

$$R = \left|\boldsymbol{R}_{0,1}\right| = \frac{\left|\boldsymbol{A'}_0 \cdot \boldsymbol{A'}_0\right|}{\left|\boldsymbol{A}_0 \cdot \boldsymbol{A}_0\right|}, \tag{28}$$

then

$$\begin{aligned} R = {} & \Psi_{0,1,xx}\Psi^*_{0,1,xx}\sin^2\chi\sin^2\theta \\ & + \Psi_{0,1,yy}\Psi^*_{0,1,yy}\cos^2\chi + \Psi_{0,1,zz}\Psi^*_{0,1,zz}\sin^2\chi\cos^2\theta \end{aligned} \tag{29}$$

where,

$$\begin{aligned} \Psi_{0,1,xx} &= \frac{k_{1,z}n_0^{\,2} - k_{0,z}n_1^{\,2}}{k_{0,z}n_1^{\,2} + k_{1,z}n_0^{\,2}} \\ \Psi_{0,1,yy} &= \frac{k_{0,z} - k_{1,z}}{k_{0,z} + k_{1,z}} \\ \Psi_{0,1,zz} &= -\frac{k_{1,z}n_0^{\,2} - k_{0,z}n_1^{\,2}}{k_{0,z}n_1^{\,2} + k_{1,z}n_0^{\,2}} \end{aligned}, \tag{30}$$

$$\begin{aligned} \Psi_{0,1,xx}\Psi^*_{0,1,xx} &= \frac{-k_{0,z}n_1^{\,2} + k_{1,z}}{k_{0,z}n_1^{\,2} + k_{1,z}} \frac{-k_{0,z}n^{*}_{1}{}^{2} + k^{*}_{1,z}}{k_{0,z}n^{*}_{1}{}^{2} + k^{*}_{1,z}} \\ \Psi_{0,1,yy}\Psi^*_{0,1,yy} &= \frac{k_{0,z} - k_{1,z}}{k_{0,z} + k_{1,z}} \frac{k_{0,z} - k^{*}_{1,z}}{k_{0,z} + k^{*}_{1,z}} \\ \Psi_{0,1,zz}\Psi^*_{0,1,zz} &= \frac{k_{0,z}n_1^{\,2} - k_{1,z}}{k_{0,z}n_1^{\,2} + k_{1,z}} \frac{k_{0,z}n^{*}_{1}{}^{2} - k^{*}_{1,z}}{k_{0,z}n^{*}_{1}{}^{2} + k^{*}_{1,z}} \\ &= \Psi_{0,1,xx}\Psi^*_{0,1,xx} \end{aligned}, \tag{31}$$

then,

$$R = \Psi_{0,1,yy}\Psi^*_{0,1,yy}\cos^2\chi + \Psi_{0,1,zz}\Psi^*_{0,1,zz}\sin^2\chi, \tag{32}$$

Taking an average for χ,

$$R = \left\langle \Psi_{0,1,yy}\Psi^*_{0,1,yy}\cos^2\chi + \Psi_{0,1,zz}\Psi^*_{0,1,zz}\sin^2\chi \right\rangle_\chi, \tag{33}$$

then

$$R = (\Psi_{0,1,yy}\Psi^*_{0,1,yy} + \Psi_{0,1,zz}\Psi^*_{0,1,zz})/2, \tag{34}$$

For the reflectivity in the case of *s*-polarized x-rays incident,

$$R = \Psi_{0,1,yy}\Psi^*_{0,1,yy}. \tag{35}$$

Next, we consider the reflection from a flat surface of a multilayer with flat interfaces. We consider the electric field $\boldsymbol{E}_{j\text{-}1}$ of x-rays propagating in the j-1-th layer material, the electric field $\boldsymbol{E}_j$ of x-rays propagating in the j-th layer material, and the electric field $\boldsymbol{E'}_{j\text{-}1}$ of x-rays reflected from the j-th layer material at $z=z_{j\text{-}1,j}$ of the interface between the j-1-th layer and j-th layers as shown in Figure 2.

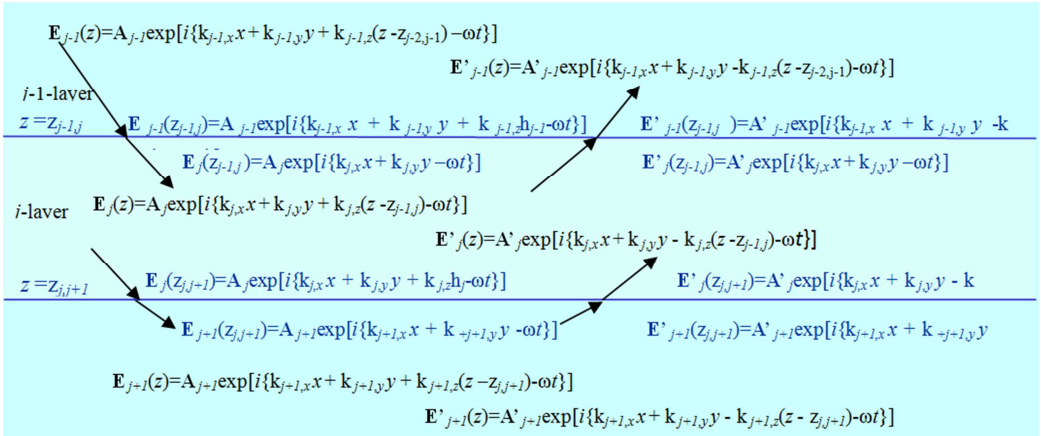

Figure 2. *Reflection and transmission of x-rays in the j-1-th, j-th, and j+1-th layers of a multilayer material.*

The electric fields $\boldsymbol{E}_{j\text{-}1}$, $\boldsymbol{E'}_{j\text{-}1}$ at the interface between the j-1-th layer and j-th layer and the electric fields $\boldsymbol{E}_j$, $\boldsymbol{E'}_j$ below the interface between the j-1-th layer and j-th layer are expressed as

$$\begin{aligned}
\boldsymbol{E}_{j-1}(z_{j-1,j}) &= \boldsymbol{A}_{j-1}\exp[\,i(k_{j-1,x}x+k_{j-1,y}y+k_{j-1,z}h_{j-1}-\omega t)\,],\\
\boldsymbol{E}'_{j-1}(z_{j-1,j}) &= \boldsymbol{A}'_{j-1}\exp[\,i(k_{j-1,x}x+k_{j-1,y}y-k_{j-1,z}h_{j-1}-\omega t)\,],\\
\boldsymbol{E}_{j}(z_{j-1,j}) &= \boldsymbol{A}_{j}\exp[\,i(k_{j,x}x+k_{j,y}y-\omega t)\,],\\
\boldsymbol{E}'_{j}(z_{j-1,j}) &= \boldsymbol{A}'_{j}\exp[\,i(k_{j,x}x+k_{j,y}y-\omega t)\,].
\end{aligned} \tag{36}$$

The electric fields of x-rays at the interface between the j-1-th layer and j-th layer can be formally expressed as follows

$$\boldsymbol{E}_j(z_{j-1,j}) = \boldsymbol{\Phi}_{j-1,j}\boldsymbol{E}_{j-1}(z_{j-1,j}) + \boldsymbol{\Psi}_{j,j-1}\boldsymbol{E'}_j(z_{j-1,j}), \tag{37}$$

$$\boldsymbol{E'}_{j-1}(z_{j-1,j}) = \boldsymbol{\Psi}_{j-1,j}\boldsymbol{E}_{j-1}(z_{j-1,j}) + \boldsymbol{\Phi}_{j,j-1}\boldsymbol{E'}_j(z_{j-1,j}), \tag{38}$$

where $\boldsymbol{\Psi}_{j\text{-}1,j}$ is the Fresnel coefficient tensor for reflection from the interface between the j-1 and j layers, and $\boldsymbol{\Phi}_{j\text{-}1,j}$ is the Fresnel coefficient tensor for refraction at the interface between the j-1 and j layers. In addition, the electric field within the j-th layer varies with depth h_j as follows

$$\boldsymbol{E}_j(z_{j,j+1}) = \boldsymbol{E}_j(z_{j-1,j})\exp(ik_{j,z}h_j), \tag{39}$$

$$\boldsymbol{E'}_j(z_{j,j+1}) = \boldsymbol{E'}_j(z_{j-1,j})\exp(-ik_{j,z}h_j). \tag{40}$$

The amplitudes A_j and A'_j at the j-th layer are derived from the above equations for the interface between the j-1 and j layers as follows

$$\boldsymbol{A}'_{j-1}\exp(-ik_{j-1,z}h_{j-1}) = \boldsymbol{\Psi}_{j-1,j}\boldsymbol{A}_{j-1}\exp(ik_{j-1,z}h_{j-1}) + \boldsymbol{\Phi}_{j,j-1}\boldsymbol{A'}_j, \tag{41}$$

$$\boldsymbol{A}_j = \boldsymbol{\Phi}_{j-1,j}\boldsymbol{A}_{j-1}\exp(ik_{j-1,z}h_{j-1}) + \boldsymbol{\Psi}_{j,j-1}\boldsymbol{A'}_j \tag{42}$$

This relation is expressed by the following matrix

$$\begin{pmatrix}\boldsymbol{A}'_{j-1}\exp(-ik_{j-1,z}h_{j-1})\\ \boldsymbol{A}_j\end{pmatrix} = \begin{pmatrix}\boldsymbol{\Psi}_{j-1,j} & \boldsymbol{\Phi}_{j,j-1}\\ \boldsymbol{\Phi}_{j-1,j} & \boldsymbol{\Psi}_{j,j-1}\end{pmatrix}\begin{pmatrix}\boldsymbol{A}_{j-1}\exp(ik_{j-1,z}h_{j-1})\\ \boldsymbol{A'}_j\end{pmatrix}, \tag{43}$$

Here, the Fresnel coefficient tensor $\boldsymbol{\Phi}$ for refraction at the interface between the j-1-th and j-th layers is given by

$$\begin{aligned}
\Phi_{j-1,j,xx} &= \frac{2k_{j,z}\boldsymbol{k}_{j\text{-}1}\cdot\boldsymbol{k}_{j-1}}{k_{j\text{-}1,z}\boldsymbol{k}_j\cdot\boldsymbol{k}_j + k_{j,z}\boldsymbol{k}_{j\text{-}1}\cdot\boldsymbol{k}_{j-1}} & \Phi_{j,j-1,xx} &= \frac{2k_{j-1,z}\boldsymbol{k}_j\cdot\boldsymbol{k}_j}{k_{j\text{-}1,z}\boldsymbol{k}_j\cdot\boldsymbol{k}_j + k_{j,z}\boldsymbol{k}_{j\text{-}1}\cdot\boldsymbol{k}_{j\text{-}1}}\\
\Phi_{j-1,j,yy} &= \frac{2k_{j\text{-}1,z}}{k_{j\text{-}1,z}+k_{j,z}} & \Phi_{j,j-1,yy} &= \frac{2k_{j,z}}{k_{j,z}+k_{j\text{-}1,z}}\\
\Phi_{j-1,j,zz} &= \frac{2k_{j\text{-}1,z}\boldsymbol{k}_{j\text{-}1}\cdot\boldsymbol{k}_{j\text{-}1}}{k_{j\text{-}1,z}\boldsymbol{k}_j\cdot\boldsymbol{k}_j + k_{j,z}\boldsymbol{k}_{j\text{-}1}\cdot\boldsymbol{k}_{j\text{-}1}} & \Phi_{j,j-1,zz} &= \frac{2k_{j,z}\boldsymbol{k}_j\cdot\boldsymbol{k}_j}{k_{j\text{-}1,z}\boldsymbol{k}_j\cdot\boldsymbol{k}_j + k_{j,z}\boldsymbol{k}_{j\text{-}1}\cdot\boldsymbol{k}_{j\text{-}1}}\\
\Phi_{j-1,j,xy} &= \Phi_{j-1,j,yx} = \Phi_{j-1,j,yz} = 0 & \Phi_{j,j-1,xy} &= \Phi_{j,j-1,yx} = \Phi_{j,j-1,yz} = 0\\
\Phi_{j-1,j,zy} &= \Phi_{j-1,j,zx} = \Phi_{j-1,j,xz} = 0 & \Phi_{j,j-1,zy} &= \Phi_{j,j-1,zx} = \Phi_{j,j-1,xz} = 0
\end{aligned} \tag{44}$$

The Fresnel coefficient tensor $\boldsymbol{\Psi}$ for reflection from the interface between the j-1 and j layers is given by

$$\begin{aligned}
\Psi_{j-1,j,xx} &= \frac{k_{j,z}\boldsymbol{k}_{j\text{-}1}\cdot\boldsymbol{k}_{j-1} - k_{j-1,z}\boldsymbol{k}_j\cdot\boldsymbol{k}_j}{k_{j\text{-}1,z}\boldsymbol{k}_j\cdot\boldsymbol{k}_j + k_{j,z}\boldsymbol{k}_{j\text{-}1}\cdot\boldsymbol{k}_{j-1}} & \Psi_{j,j-1,xx} &= \frac{k_{j-1,z}\boldsymbol{k}_j\cdot\boldsymbol{k}_j - k_{j,z}\boldsymbol{k}_{j\text{-}1}\cdot\boldsymbol{k}_{j\text{-}1}}{k_{j\text{-}1,z}\boldsymbol{k}_j\cdot\boldsymbol{k}_j + k_{j,z}\boldsymbol{k}_{j\text{-}1}\cdot\boldsymbol{k}_{j\text{-}1}}\\
\Psi_{j-1,j,yy} &= \frac{k_{j\text{-}1,z}-k_{j,z}}{k_{j\text{-}1,z}+k_{j,z}} & \Psi_{j,j-1,yy} &= \frac{k_{j,z}-k_{j\text{-}1,z}}{k_{j\text{-}1,z}+k_{j,z}}\\
\Psi_{j-1,j,zz} &= -\frac{k_{j,z}\boldsymbol{k}_{j\text{-}1}\cdot\boldsymbol{k}_{j\text{-}1} - k_{j\text{-}1,z}\boldsymbol{k}_j\cdot\boldsymbol{k}_j}{k_{j\text{-}1,z}\boldsymbol{k}_j\cdot\boldsymbol{k}_j + k_{j,z}\boldsymbol{k}_{j\text{-}1}\cdot\boldsymbol{k}_{j\text{-}1}} & \Psi_{j,j-1,zz} &= \frac{k_{j,z}\boldsymbol{k}_{j\text{-}1}\cdot\boldsymbol{k}_{j\text{-}1} - k_{j\text{-}1,z}\boldsymbol{k}_j\cdot\boldsymbol{k}_j}{k_{j\text{-}1,z}\boldsymbol{k}_j\cdot\boldsymbol{k}_j + k_{j,z}\boldsymbol{k}_{j\text{-}1}\cdot\boldsymbol{k}_{j\text{-}1}}\\
\Psi_{j-1,j,xy} &= \Psi_{j-1,j,yx} = \Psi_{j-1,j,yz} = 0 & \Psi_{j,j-1,xy} &= \Psi_{j,j-1,yx} = \Psi_{j,j-1,yz} = 0\\
\Psi_{j-1,j,zy} &= \Psi_{j-1,j,zx} = \Psi_{j-1,j,xz} = 0 & \Psi_{j,j-1,zy} &= \Psi_{j,j-1,zx} = \Psi_{j,j-1,xz} = 0
\end{aligned} \tag{45}$$

The amplitudes $\boldsymbol{A}_{j\text{-}1}$ and $\boldsymbol{A}'_{j\text{-}1}$ of the electric fields $\boldsymbol{E}_{j\text{-}1}$, $\boldsymbol{E'}_{j\text{-}1}$ at the j-th layer and the amplitudes $\boldsymbol{A}_j$ and $\boldsymbol{A}'_j$ of the electric fields $\boldsymbol{E}_j$, $\boldsymbol{E'}_j$ at the j+1-th layer are related by the following equations;

$$\begin{pmatrix}\boldsymbol{\Phi}_{j-1,j} & 0\\ 0 & \boldsymbol{\Phi}_{j-1,j}\end{pmatrix}\begin{pmatrix}\boldsymbol{A}_{j-1}\\ \boldsymbol{A}'_{j-1}\end{pmatrix} = \begin{pmatrix}\exp(-ik_{j-1,z}h_{j-1}) & 0\\ 0 & \exp(ik_{j-1,z}h_{j-1})\end{pmatrix}\begin{pmatrix}1 & -\boldsymbol{\Psi}_{j,j-1}\\ \boldsymbol{\Psi}_{j-1,j} & (\boldsymbol{\Phi}_{j-1,j}\boldsymbol{\Phi}_{j,j-1} - \boldsymbol{\Psi}_{j-1,j}\boldsymbol{\Psi}_{j,j-1})\end{pmatrix}\begin{pmatrix}\boldsymbol{A}_j\\ \boldsymbol{A}'_j\end{pmatrix}, \tag{46}$$

For s-polarization, the Fresnel coefficients are,

$$\Phi_{j-1,j,yy} = \frac{2k_{j\text{-}1,z}}{k_{j\text{-}1,z}+k_{j,z}} \quad , \quad \Phi_{j,j-1,yy} = \frac{2k_{j,z}}{k_{j\text{-}1,z}+k_{j,z}} \tag{47}$$

$$\Psi_{j-1,j,yy} = \frac{k_{j\text{-}1,z}-k_{j,z}}{k_{j\text{-}1,z}+k_{j,z}} \quad , \quad \Psi_{j,j-1,yy} = \frac{k_{j,z}-k_{j-1,z}}{k_{j\text{-}1,z}+k_{j,z}} \tag{48}$$

Then, the relations between the amplitudes $A_{j\text{-}1}$, $A'_{j\text{-}1}$, A_j, and A'_j at the interface of the j-1-th and j-th layers are expressed as follows,

$$\begin{pmatrix}A_{j-1}\\ A'_{j-1}\end{pmatrix} = \begin{pmatrix}\exp(-ik_{j-1,z}h_{j-1}) & 0\\ 0 & \exp(ik_{j-1,z}h_{j-1})\end{pmatrix}\begin{pmatrix}\dfrac{k_{j\text{-}1,z}+k_{j,z}}{2k_{j\text{-}1,z}} & \dfrac{k_{j\text{-}1,z}-k_{j,z}}{2k_{j\text{-}1,z}}\\ \dfrac{k_{j\text{-}1,z}-k_{j,z}}{2k_{j\text{-}1,z}} & \dfrac{k_{j\text{-}1,z}+k_{j,z}}{2k_{j\text{-}1,z}}\end{pmatrix}\begin{pmatrix}A_j\\ A'_j\end{pmatrix} \tag{49}$$

The reflection coefficient is defined as the ratio $\boldsymbol{R}_{o,1}$ of the reflected electric field to the incident electric field at the surface of the material and is given by,

$$\boldsymbol{A'}_0 = \boldsymbol{R}_{0,1}\boldsymbol{A}_0. \tag{50}$$

The reflection coefficient $\boldsymbol{R}_{j\text{-}1,j}$ of the electric field $\boldsymbol{E'}_{j\text{-}1}$ to the electric field $\boldsymbol{E}_{j\text{-}1}$ at the interface of j-1-th layer and j-th layer is,

$$\boldsymbol{A'}_{j\text{-}1} = \boldsymbol{R}_{j-1,j}\boldsymbol{A}_{j-1}, \tag{51}$$

and the ratio $R_{j\text{-}1,j}$ is related to the ratio $R_{j,j+1}$ as follows,

$$\boldsymbol{R}_{j-1,j} = \frac{\boldsymbol{\Psi}_{j-1,j} + (\boldsymbol{\Phi}_{j-1,j}\boldsymbol{\Phi}_{j,j-1} - \boldsymbol{\Psi}_{j-1,j}\boldsymbol{\Psi}_{j,j-1})\boldsymbol{R}_{j,j+1}}{1-\boldsymbol{\Psi}_{j,j-1}\boldsymbol{R}_{j,j+1}}\exp(2ik_{j-1,z}h_{j-1}) \tag{52}$$

Here, from the relation between the Fresnel coefficient for reflection and the Fresnel coefficient for refraction,

$$\boldsymbol{\Phi}_{j-1,j}\boldsymbol{\Phi}_{j,j-1} - \boldsymbol{\Psi}_{j-1,j}\boldsymbol{\Psi}_{j,j-1} = 1, \quad (53)$$

$$\boldsymbol{\Psi}_{j-1,j} = -\boldsymbol{\Psi}_{j,j-1} \quad (54)$$

we can formulate the following relationship

$$\boldsymbol{R}_{j-1,j} = \frac{\boldsymbol{\Psi}_{j-1,j} + \boldsymbol{R}_{j,j+1}}{1 + \boldsymbol{\Psi}_{j-1,j}\boldsymbol{R}_{j,j+1}} \exp(2ik_{j-1,z}h_{j-1}) \quad (55)$$

It is reasonable to assume that no wave will be reflected back from the substrate, so that,

$$\boldsymbol{R}_{N,N+1} = 0 \quad (56)$$

Then, the x-ray reflectivity is simply,

$$R = \left|R_{0,1}\right|^2 \quad (57)$$

2.2. Previous Calculations of X-ray Reflectivity When Roughness Exists at the Surface and Interface

When the surface and interface have roughness, the Fresnel coefficient for reflection is reduced by the roughness. [15-18, 20-23] The effect of the roughness was previously put into the calculation based on the theory of Nevot and Croce. [2] The effect of such roughness was taken into account only through the effect of the changes in density of the medium in a vertical direction to the surface and interface. With the use of relevant roughness parameters like the root-mean-square (rms) roughness $\sigma_{j-1,j}$ of the j-th layer, the reduced Fresnel reflection coefficient Ψ' for s-polarization is transformed as shown below,

$$\Psi'_{j-1,j} = \frac{k_{j-1,z} - k_{j,z}}{k_{j-1,z} + k_{j,z}} \exp\left(-2k_{j-1,z}k_{j,z}\sigma_{j-1,j}^{\ 2}\right), \quad \Psi'_{j,j-1} = -\Psi'_{j-1,j}, \quad (58)$$

and the x-ray reflectivity is calculated using the following equation,

$$R = \left|R_{0,1}\right|^2, \quad R_{j-1,j} = \frac{\Psi'_{j-1,j} + R_{j,j+1}}{1 - \Psi'_{j,j-1}R_{j,j+1}} \exp(2ik_{j-1,z}h_{j-1}), \quad R_{N,N+1} = 0. \quad (59)$$

Figure 3 shows the reflectivity from a GaAs-covered silicon wafer, solid line shows the calculated result in the case of flat surface and flat interface, dashed line shows the calculated result in the case that the surface has an rms roughness of 4 nm, and dotted line shows the equivalent result when the surface and interface both have an rms roughness of 4 nm. In the latter case, the reflectivity curve (dots) decreases more quickly than that in Figure 3. However, the ratio of the oscillation amplitude to the value of the reflectivity does not decrease. It seems unnatural that the effect of interference does not also decrease at a rough surface and interface, because the amount of coherent x-rays should reduce due to diffuse scattering at a rough surface and interface.

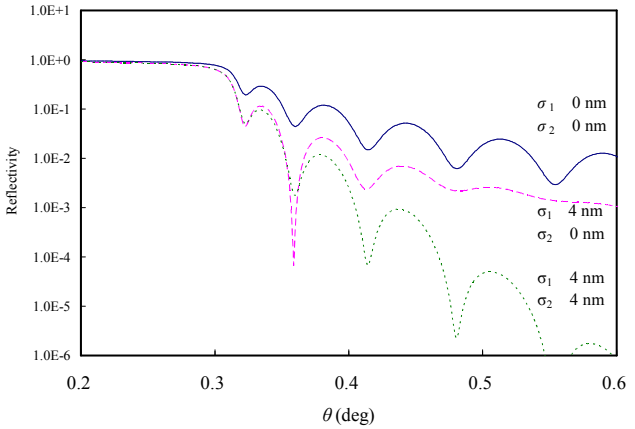

Figure 3. *Calculated reflectivity from a GaAs layer with a thickness of 48 nm on a Si substrate. The solid curve is for a flat surface and a flat interface. The dashed curve is for a surface roughness σ_1 of 4 nm and a flat interface, while the dotted curve is for a surface roughness σ_1 of 4 nm and interface roughness σ_2 of 4 nm.*

In the reflectivity curve (dashed line) for a surface roughness of 4 nm and with a flat interface, the ratio of the oscillation amplitude to the size of the reflectivity near an angle of incidence of 0.36° is much larger than the reflectivity of the flat surface in Figure 1. It seems very strange that the interference effects would increase so much at a rough surface.

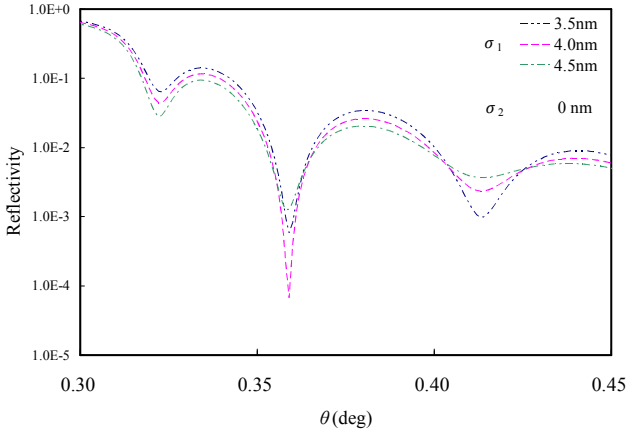

Figure 4. *Calculated reflectivity from a GaAs layer with a thickness of 48 nm on a Si substrate. In the calculation, the interface roughness σ_2 is 0 nm. Three calculated results are shown for a GaAs surface with an rms roughness σ_1 of 3.5 nm, 4 nm, and 4.5 nm.*

To probe these effects further, we then recalculated the reflectivity for surface roughness of 3.5 nm, 4 nm, and 4.5 nm, and with a flat interface. Those calculated reflectivity results are shown in Figure 4. The ratio of the oscillation amplitude to the reflectivity near an angle of incidence of 0.36° in calculated reflectivity is larger in all cases than that of the reflectivity in the case of a flat surface in Figure 1.

For most angles of incidence within this range, the reflectivity of the surface with a roughness of 4 nm is near the mean value of the reflectivity of surfaces with roughnesses of 3.5 nm and 4.5 nm. However, near an angle of incidence of 0.36°, the reflectivity of the surface with a

roughness of 4 nm is very much attenuated compared to that same average. It seems very strange that the reflectivity of the average roughness has a value quite different from the mean value of the reflectivity of each roughness, because the value of the roughness is not the value of the amplitude of a rough surface but the standard deviation value of various amplitudes of rough surface.

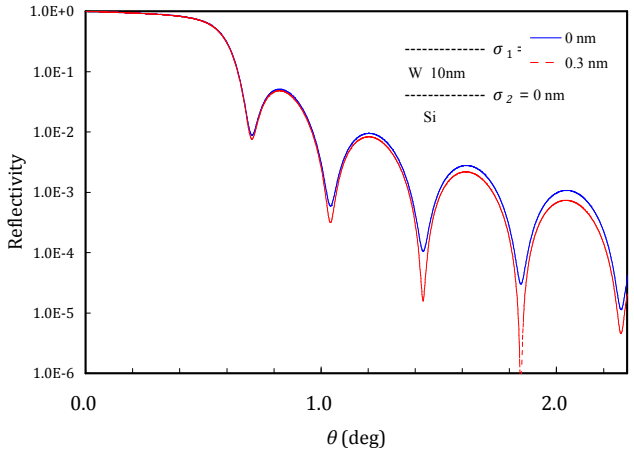

Figure 5. *X-ray reflectivity from a silicon wafer covered with a thin (10 nm) tungsten film calculated by the theory in use prior to this work. Solid line shows the case of a flat surface. Dashed line shows the case of a surface with an rms surface roughness of 0.3 nm.*

Figure 5 shows the reflectivity from a tungsten-covered silicon wafer calculated by the theory in use prior to this work. The ratio of the oscillation amplitude to the value of the reflectivity from a surface with a rms surface roughness of 0.3 nm (dashed line) does not decrease near an angle of incidence of 1.8° but increase. This result is strange and not reasonable.

2.3. Effect of Roughness on X-ray Reflectivity of Multilayer Surface

We now consider the above strange result of the x-ray reflectivity which was calculated based on the Parratt formalism [1] with the use of the Nevot and Croce approach to account for roughness. [2] In that calculation, the x-ray reflectivity is derived using the relation of the reflection coefficient $R_{j\text{-}1,j}$ and $R_{j,j+1}$ as follows,

$$R_{j-1,j} = \frac{R_{j,j+1} + \Psi'_{j-1,j}}{1 + R_{j,j+1}\Psi'_{j-1,j}} \exp(2ik_{j-1,z}h_{j-1}), \tag{60}$$

where the reduced Fresnel reflection coefficient Ψ' that takes into account the effect of the roughness is as shown below,

$$\Psi'_{j,j-1} = \Psi_{j,j-1} \exp(-2k_{j,z}k_{j-1,z}\sigma^2_{j,j-1}). \tag{61}$$

However, the relationship between the reflection coefficients $R_{j\text{-}1,j}$ and $R_{j,j+1}$ was originally derived as the following equation,

$$\boldsymbol{R}_{j-1,j} = \frac{\boldsymbol{\Psi}'_{j-1,j} + (\boldsymbol{\Phi}'_{j-1,j}\boldsymbol{\Phi}'_{j,j-1} - \boldsymbol{\Psi}'_{j-1,j}\boldsymbol{\Psi}'_{j,j-1})\boldsymbol{R}_{j,j+1}}{1 - \boldsymbol{\Psi}'_{j,j-1}\boldsymbol{R}_{j,j+1}} \exp(2ik_{j-1,z}h_{j-1}), \tag{62}$$

Here, the following conditional relations between the Fresnel coefficient for reflection and refraction are relevant to the above equation,

$$\boldsymbol{\Phi}'_{j-1,j}\boldsymbol{\Phi}'_{j,j-1} - \boldsymbol{\Psi}'_{j-1,j}\boldsymbol{\Psi}'_{j,j-1} = 1, \tag{63}$$

and,

$$\boldsymbol{\Psi}'_{j-1,j} = -\boldsymbol{\Psi}'_{j,j-1}. \tag{64}$$

then,

$$\boldsymbol{\Phi}'_{j-1,j}\boldsymbol{\Phi}'_{j,j-1} + \boldsymbol{\Psi}'^2_{j,j-1} = 1, \tag{65}$$

i.e.,

$$\boldsymbol{\Phi}'_{j-1,j}\boldsymbol{\Phi}'_{j,j-1} = 1 - \boldsymbol{\Psi}'^2_{j,j-1}. \tag{66}$$

The Fresnel coefficients for refraction at the rough interface are derived using the Fresnel reflection coefficient Ψ as follows,

$$\boldsymbol{\Phi}'_{j-1,j}\boldsymbol{\Phi}'_{j,j-1} - \boldsymbol{\Phi}_{j-1,j}\boldsymbol{\Phi}_{j,j-1} = \boldsymbol{\Psi}^2_{j,j-1}\left(1 - \exp(-2k_{j,z}k_{j-1,z}\sigma^2_{j,j-1})\right) > 0, \tag{67}$$

$$\boldsymbol{\Phi}'_{j-1,j}\boldsymbol{\Phi}'_{j,j-1} = \boldsymbol{\Phi}_{j-1,j}\boldsymbol{\Phi}_{j,j-1} + \left(1 - \boldsymbol{\Phi}_{j-1,j}\boldsymbol{\Phi}_{j,j-1}\right)\left(1 - \exp(-2k_{j,z}k_{j-1,z}\sigma^2_{j,j-1})\right). \tag{68}$$

Therefore, the Fresnel coefficients for refraction at the rough interface are necessarily larger than the Fresnel coefficient for refraction at the flat interface. The resulting increase in the transmission coefficient completely overpowers any decrease in the value of the reflection coefficient. These coefficients for refraction obviously contain a mistake because the penetration of x-rays should decrease at a rough interface because of diffuse scattering.

We propose that the unnatural results in the previous calculation of the x-ray reflectivity originate from the fact that diffuse scattering was not considered. In fact equation (63) contains the x-ray energy conservation rule at the interface as the following identity equation for the Fresnel coefficient,

$$\Phi_{j-1,j}\Phi_{j,j-1}-\Psi_{j-1,j}\Psi_{j,j-1}=\Phi_{j-1,j}\Phi_{j,j-1}+\Psi_{j-1,j}{}^{2}=1. \quad (69)$$

Here, we consider the energy flow of the x-ray. In electromagnetic radiation, $\boldsymbol{E}$, $\boldsymbol{H}$, the energy flow is equal to the Poynting vector

$$\boldsymbol{p}=\frac{1}{4}\left(\boldsymbol{E}^{*}\times\boldsymbol{H}+\boldsymbol{E}\times\boldsymbol{H}^{*}\right), \quad (70)$$

where

$$\boldsymbol{H}=\sqrt{\frac{\varepsilon}{\mu}}\frac{\boldsymbol{k}}{k}\times\boldsymbol{E}, \quad (71)$$

and ε and μ are the dielectric and magnetic permeability. The Poynting vector is therefore

$$\boldsymbol{p}=\frac{1}{4}\sqrt{\frac{\varepsilon}{\mu}}\left(\boldsymbol{E}^{*}\times\left(\frac{\boldsymbol{k}}{k}\times\boldsymbol{E}\right)+\boldsymbol{E}\times\left(\frac{\boldsymbol{k}}{k}\times\boldsymbol{E}\right)^{*}\right)=\frac{1}{4}\sqrt{\frac{\varepsilon}{\mu}}\left(\frac{\boldsymbol{k}}{k}\boldsymbol{E}^{*}\cdot\boldsymbol{E}+\frac{\boldsymbol{k}^{*}}{k}\boldsymbol{E}\cdot\boldsymbol{E}^{*}\right)=\frac{1}{2\varpi\mu}\frac{\boldsymbol{k}+\boldsymbol{k}^{*}}{2}|\boldsymbol{E}|^{2}. \quad (72)$$

Then, the Poynting vector that crosses the interface is

$$\int \boldsymbol{p}d\boldsymbol{S}=\int\frac{1}{2\mu\omega}\frac{\boldsymbol{k}+\boldsymbol{k}^{*}}{2}|\boldsymbol{E}|^{2}d\boldsymbol{S}=\frac{1}{2\mu\omega}\int\frac{\boldsymbol{k}+\boldsymbol{k}^{*}}{2}|\boldsymbol{E}|^{2}d\boldsymbol{S}=\frac{1}{2\mu\omega}\frac{k_{z}+k_{z}^{*}}{2}|\boldsymbol{A}|^{2}. \quad (73)$$

The amplitudes $\boldsymbol{A}_{j\text{-}1}$ and $\boldsymbol{A}'_{j\text{-}1}$ of the electric fields $\boldsymbol{E}_{j\text{-}1}$, $\boldsymbol{E}'_{j\text{-}1}$ at the j-th layer and amplitudes $\boldsymbol{A}_{j}$ and $\boldsymbol{A}'_{j}$ of the electric fields $\boldsymbol{E}_{j}$, $\boldsymbol{E}'_{j}$ at the j+1-th layer are related by the following equations;

$$\begin{pmatrix}\boldsymbol{\Phi}_{j-1,j} & 0\\ 0 & \boldsymbol{\Phi}_{j-1,j}\end{pmatrix}\begin{pmatrix}\boldsymbol{A}_{j-1}\\ \boldsymbol{A}'_{j-1}\end{pmatrix}=\begin{pmatrix}\exp(-ik_{j-1,z}h_{j-1}) & 0\\ 0 & \exp(ik_{j-1,z}h_{j-1})\end{pmatrix}\begin{pmatrix}1 & -\boldsymbol{\Psi}_{j,j-1}\\ \boldsymbol{\Psi}_{j-1,j} & \left(\boldsymbol{\Phi}_{j-1,j}\boldsymbol{\Phi}_{j,j-1}-\boldsymbol{\Psi}_{j-1,j}\boldsymbol{\Psi}_{j,j-1}\right)\end{pmatrix}\begin{pmatrix}\boldsymbol{A}_{j}\\ \boldsymbol{A}'_{j}\end{pmatrix}, \quad (74)$$

When

$$\boldsymbol{\Phi}_{j-1,j}\boldsymbol{\Phi}_{j,j-1}-\boldsymbol{\Psi}_{j-1,j}\boldsymbol{\Psi}_{j,j-1}=1,\ \boldsymbol{\Psi}_{j-1,j}=-\boldsymbol{\Psi}_{j,j-1}, \quad (75)$$

we can describe the above equation as,

$$\begin{pmatrix}\boldsymbol{\Phi}_{j-1,j} & 0\\ 0 & \boldsymbol{\Phi}_{j-1,j}\end{pmatrix}\begin{pmatrix}\boldsymbol{A}_{j-1} & \boldsymbol{A}'^{*}{}_{j-1}\\ \boldsymbol{A}'_{j-1} & \boldsymbol{A}^{*}{}_{j-1}\end{pmatrix}=\begin{pmatrix}\exp(-ik_{j-1,z}h_{j-1}) & 0\\ 0 & \exp(ik_{j-1,z}h_{j-1})\end{pmatrix}\begin{pmatrix}1 & \boldsymbol{\Psi}_{j-1,j}\\ \boldsymbol{\Psi}_{j-1,j} & 1\end{pmatrix}\begin{pmatrix}\boldsymbol{A}_{j} & \boldsymbol{A}'^{*}{}_{j}\\ \boldsymbol{A}'_{j} & \boldsymbol{A}^{*}{}_{j}\end{pmatrix}, \quad (76)$$

From the determinant of the refraction matrix,

$$\begin{vmatrix}\boldsymbol{\Phi}_{j-1,j} & 0\\ 0 & \boldsymbol{\Phi}_{j-1,j}\end{vmatrix}\left(|\boldsymbol{A}_{j-1}|^{2}-|\boldsymbol{A}'_{j-1}|^{2}\right)=\begin{vmatrix}\exp(-ik_{j-1,z}h_{j-1}) & 0\\ 0 & \exp(ik_{j-1,z}h_{j-1})\end{vmatrix}\begin{vmatrix}1 & \boldsymbol{\Psi}_{j-1,j}\\ \boldsymbol{\Psi}_{j-1,j} & 1\end{vmatrix}\left(|\boldsymbol{A}_{j}|^{2}-|\boldsymbol{A}'_{j}|^{2}\right), \quad (77)$$

then

$$\boldsymbol{\Phi}^{2}{}_{j-1,j}\left(|\boldsymbol{A}_{j-1}|^{2}-|\boldsymbol{A}'_{j-1}|^{2}\right)=\left(1-\boldsymbol{\Psi}^{2}{}_{j-1,j}\right)\left(|\boldsymbol{A}_{j}|^{2}-|\boldsymbol{A}'_{j}|^{2}\right), \quad (78)$$

$$\boldsymbol{\Phi}_{j-1,j}\left(|\boldsymbol{A}_{j-1}|^{2}-|\boldsymbol{A}'_{j-1}|^{2}\right)=\boldsymbol{\Phi}_{j,j-1}\left(|\boldsymbol{A}_{j}|^{2}-|\boldsymbol{A}'_{j}|^{2}\right), \quad (79)$$

$$\frac{2k_{j\text{-}1,z}}{k_{j\text{-}1,z}+k_{j,z}}\left(|\boldsymbol{A}_{j-1}|^{2}-|\boldsymbol{A}'_{j-1}|^{2}\right)=\frac{2k_{j,z}}{k_{j\text{-}1,z}+k_{j,z}}\left(|\boldsymbol{A}_{j}|^{2}-|\boldsymbol{A}'_{j}|^{2}\right), \quad (80)$$

$$k_{j\text{-}1,z}|\boldsymbol{A}_{j-1}|^{2}-k_{j\text{-}1,z}|\boldsymbol{A}'_{j-1}|^{2}=k_{j,z}|\boldsymbol{A}_{j}|^{2}-k_{j,z}|\boldsymbol{A}'_{j}|^{2}, \quad (81)$$

i.e., the x-ray energy flow is conserved at the interface. When the Fresnel coefficients at the rough interface obeys the following equations,

$$\boldsymbol{\Phi}'_{j-1,j}\boldsymbol{\Phi}'_{j,j-1}-\boldsymbol{\Psi}'_{j-1,j}\boldsymbol{\Psi}'_{j,j-1}=1,\ \boldsymbol{\Psi}'_{j-1,j}=-\boldsymbol{\Psi}'_{j,j-1}, \quad (82)$$

these coefficients fulfil x-ray energy flow conservation at the interface, and so diffuse scattering was not considered at the rough interface.

This conservation expression should not apply any longer when the Fresnel reflection coefficient is replaced by the reduced coefficient $\boldsymbol{\Psi}'$ when there is roughening at the interface. Therefore, calculating the reflectivity using this reduced Fresnel reflection coefficient $\boldsymbol{\Psi}'$ in equation (61) will incorrectly increase the Fresnel transmission coefficient $\boldsymbol{\Phi}'$, *i.e.*, $\Phi<\Phi'$.

The penetration of x-rays should decrease at a rough interface because of diffuse scattering. Therefore, the identity equation for the Fresnel coefficients become,

$$\Phi'_{j-1,j}\Phi'_{j,j-1}-\Psi'_{j-1,j}\Psi'_{j,j-1}=\Phi'_{j-1,j}\Phi'_{j,j-1}+\Psi'_{j-1,j}{}^{2}=1-D^{2}<1. \tag{83}$$

where D^2 is a decrease due to diffuse scattering. Then, in the calculation of x-ray reflectivity when there is roughening at the surface or the interface, the Fresnel transmission coefficient $\boldsymbol{\Phi}'$ should be used for the reduced coefficient. Several theories exist to describe the influence of roughness on x-ray scattering. [15-18, 20-23] When the surface and interface are both rough, the Fresnel coefficient for refraction has been derived in several theories. [15-18, 20-23]

2.4. The Refractive Fresnel Coefficient of a Rough Interface Used in Previous Reflectivity Calculations

Initially, we consider the reduced Fresnel coefficient, which is known as the Croce-Nevot factor. When the z position of the interface of 0-th layer and 1-th layer $z_{o,1}$ fluctuates vertically as a function of the lateral position because of the interface roughness, the relations between the amplitudes A_0, A'_0, A_1, and A'_1 are derived by the use of the Fresnel coefficient tensor $\boldsymbol{\Phi}$ for refraction and the Fresnel coefficient tensor $\boldsymbol{\Psi}$ for reflection as follows

$$\boldsymbol{A}_1\exp(ik_{1,z}z_{0,1})=\boldsymbol{\Phi}_{0,1}\boldsymbol{A}_0\exp(ik_{0,z}z_{0,1})+\boldsymbol{\Psi}_{1,0}\boldsymbol{A}'_1\exp(-ik_{1,z}z_{0,1}) \tag{84}$$

$$\boldsymbol{A}'_0\exp(-ik_{0,z}z_{0,1})=\boldsymbol{\Psi}_{0,1}\boldsymbol{A}_0\exp(ik_{0,z}z_{0,1})+\boldsymbol{\Phi}_{1,0}\boldsymbol{A}'_1\exp(-ik_{1,z}z_{0,1}) \tag{85}$$

then,

$$\begin{pmatrix}\boldsymbol{\Phi}_{0,1}\exp(ik_{0,z}z_{0,1}) & 0\\ \boldsymbol{\Psi}_{0,1}\exp(ik_{0,z}z_{0,1}) & -\exp(-ik_{0,z}z_{0,1})\end{pmatrix}\begin{pmatrix}A_0\\ A'_0\end{pmatrix}=\begin{pmatrix}\exp(ik_{1,z}z_{0,1}) & -\boldsymbol{\Psi}_{1,0}\exp(-ik_{1,z}z_{0,1})\\ 0 & -\boldsymbol{\Phi}_{1,0}\exp(-ik_{1,z}z_{0,1})\end{pmatrix}\begin{pmatrix}A_1\\ A'_1\end{pmatrix} \tag{86}$$

$$\begin{pmatrix}A_0\\ A'_0\end{pmatrix}=\frac{1}{\boldsymbol{\Phi}_{0,1}}\begin{pmatrix}\exp(-ik_{0,z}z_{0,1}) & 0\\ \boldsymbol{\Psi}_{0,1}\exp(ik_{0,z}z_{0,1}) & -\boldsymbol{\Phi}_{0,1}\exp(ik_{0,z}z_{0,1})\end{pmatrix}\begin{pmatrix}\exp(ik_{1,z}z_{0,1}) & -\boldsymbol{\Psi}_{1,0}\exp(-ik_{1,z}z_{0,1})\\ 0 & -\boldsymbol{\Phi}_{1,0}\exp(-ik_{1,z}z_{0,1})\end{pmatrix}\begin{pmatrix}A_1\\ A'_1\end{pmatrix} \tag{87}$$

$$\begin{pmatrix}A_0\\ A'_0\end{pmatrix}=\frac{1}{\boldsymbol{\Phi}_{0,1}}\begin{pmatrix}\exp(-i(k_{0,z}-k_{1,z})z_{0,1}) & -\boldsymbol{\Psi}_{1,0}\exp(-i(k_{0,z}+k_{1,z})z_{0,1})\\ \boldsymbol{\Psi}_{0,1}\exp(i(k_{0,z}+k_{1,z})z_{0,1}) & (\boldsymbol{\Phi}_{0,1}\boldsymbol{\Phi}_{1,0}-\boldsymbol{\Psi}_{0,1}\boldsymbol{\Psi}_{1,0})\exp(i(k_{0,z}-k_{1,z})z_{0,1})\end{pmatrix}\begin{pmatrix}A_1\\ A'_1\end{pmatrix} \tag{88}$$

where

$$\Psi_{0,1,yy}=\frac{k_{0,z}-k_{1,z}}{k_{0,z}+k_{1,z}},\quad \Psi_{1,0yy}=\frac{k_{1,z}-k_{0,z}}{k_{0,z}+k_{1,z}} \tag{89}$$

$$\Phi_{0,1,yy}=\frac{2k_{0,z}}{k_{0,z}+k_{1,z}},\quad \Phi_{1,0,yy}=\frac{2k_{1,z}}{k_{1,z}+k_{0,z}} \tag{90}$$

then

$$\begin{pmatrix}A_0\\ A'_0\end{pmatrix}=\begin{pmatrix}\frac{k_{0,z}+k_{1,z}}{2k_{0,z}}\exp(-i(k_{0,z}-k_{1,z})z_{0,1}) & \frac{k_{0,z}-k_{1,z}}{2k_{0,z}}\exp(-i(k_{0,z}+k_{1,z})z_{0,1})\\ \frac{k_{0,z}-k_{1,z}}{2k_{0,z}}\exp(i(k_{0,z}+k_{1,z})z_{0,1}) & \frac{k_{0,z}+k_{1,z}}{2k_{0,z}}\exp(i(k_{0,z}-k_{1,z})z_{0,1})\end{pmatrix}\begin{pmatrix}A_1\\ A'_1\end{pmatrix} \tag{91}$$

We take the average value of the matrix over the whole area coherently illuminated by the incident x-ray beam. This leads to

$$\begin{pmatrix}A_0\\ A'_0\end{pmatrix}=\begin{pmatrix}\frac{k_{0,z}+k_{1,z}}{2k_{0,z}}\left\langle\exp(-i(k_{0,z}-k_{1,z})z_{0,1})\right\rangle & \frac{k_{0,z}-k_{1,z}}{2k_{0,z}}\left\langle\exp(-i(k_{0,z}+k_{1,z})z_{0,1})\right\rangle\\ \frac{k_{0,z}-k_{1,z}}{2k_{0,z}}\left\langle\exp(i(k_{0,z}+k_{1,z})z_{0,1})\right\rangle & \frac{k_{0,z}+k_{1,z}}{2k_{0,z}}\left\langle\exp(i(k_{0,z}-k_{1,z})z_{0,1})\right\rangle\end{pmatrix}\begin{pmatrix}A_1\\ A'_1\end{pmatrix} \tag{92}$$

For Gaussian statistics of standard deviation value,

$$g(z)=\frac{1}{\sqrt{2\pi}\sigma}\exp(-\frac{z^2}{2\sigma^2}) \tag{93}$$

$$\left\langle f(z)\right\rangle=\int_{-\infty}^{\infty}g(z)f(z)dz=\int_{-\infty}^{\infty}\frac{1}{\sqrt{2\pi}\sigma}\exp(-\frac{z^2}{2\sigma^2})f(z)dz \tag{94}$$

$$\left\langle \exp(ikz_{0,1}) \right\rangle = \int_{-\infty}^{\infty} g(z_{0,1}) \exp(ikz_{0,1}) dz_{0,1} = \int_{-\infty}^{\infty} \frac{1}{\sqrt{2\pi}\sigma_{0,1}} \exp(-\frac{{z_{0,1}}^2}{2{\sigma_{0,1}}^2}) \exp(ikz_{0,1}) dz_{0,1} = \exp\left(-\frac{1}{2}k^2{\sigma_{0,1}}^2\right) \tag{95}$$

$$\begin{pmatrix} A_0 \\ A'_0 \end{pmatrix} = \begin{pmatrix} \frac{k_{0,z}+k_{1,z}}{2k_{0,z}} \exp(-\frac{1}{2}(k_{0,z}-k_{1,z})^2{\sigma_{0,1}}^2) & \frac{k_{0,z}-k_{1,z}}{2k_{0,z}} \exp(-\frac{1}{2}(k_{0,z}+k_{1,z})^2{\sigma_{0,1}}^2) \\ \frac{k_{0,z}-k_{1,z}}{2k_{0,z}} \exp(-\frac{1}{2}(k_{0,z}+k_{1,z})^2{\sigma_{0,1}}^2) & \frac{k_{0,z}+k_{1,z}}{2k_{0,z}} \exp(-\frac{1}{2}(k_{0,z}-k_{1,z})^2{\sigma_{0,1}}^2) \end{pmatrix} \begin{pmatrix} A_1 \\ A'_1 \end{pmatrix} \tag{96}$$

Therefore

$$\begin{pmatrix} A'_0 \\ A_1 \end{pmatrix} = \begin{pmatrix} \frac{k_{0,z}-k_{1,z}}{k_{0,z}+k_{1,z}} \exp(-2k_{0,z}k_{1,z}{\sigma_{0,1}}^2) & \frac{2k_{1,z}}{k_{0,z}+k_{1,z}} \exp(\frac{1}{2}(k_{0,z}-k_{1,z})^2{\sigma_{0,1}}^2) \left(\frac{(k_{0,z}+k_{1,z})^2}{4k_{0,z}k_{1,z}} \exp(-(k_{0,z}-k_{1,z})^2{\sigma_{0,1}}^2) - \frac{(k_{0,z}-k_{1,z})^2}{4k_{0,z}k_{1,z}} \exp(-(k_{0,z}+k_{1,z})^2{\sigma_{0,1}}^2) \right) \\ \frac{2k_{0,z}}{k_{0,z}+k_{1,z}} \exp(\frac{1}{2}(k_{0,z}-k_{1,z})^2{\sigma_{0,1}}^2) & \frac{k_{1,z}-k_{0,z}}{k_{0,z}+k_{1,z}} \exp(-2k_{0,z}k_{1,z}{\sigma_{0,1}}^2) \end{pmatrix} \begin{pmatrix} A_0 \\ A'_1 \end{pmatrix} \tag{97}$$

$$\begin{pmatrix} A'_0 \\ A_1 \end{pmatrix} = \begin{pmatrix} \boldsymbol{\Psi}'_{0,1} & \boldsymbol{\Phi}'_{1,0} \\ \boldsymbol{\Phi}'_{0,1} & \boldsymbol{\Psi}'_{1,0} \end{pmatrix} \begin{pmatrix} A_0 \\ A'_1 \end{pmatrix} \tag{98}$$

Then the Fresnel reflection coefficients Ψ' are reduced as follows

$$\Psi'_{0,1} = \Psi_{0,1} \exp(-2k_{0,z}k_{1,z}\sigma_{0,1}^2) \quad , \quad \Psi'_{1,0} = -\Psi_{0,1} . \tag{99}$$

However, the Fresnel refraction coefficients Φ' increase as follows

$$\boldsymbol{\Phi}'_{0,1} = \boldsymbol{\Phi}_{0,1} \exp(\frac{1}{2}(k_{0,z}-k_{1,z})^2{\sigma_{0,1}}^2) \tag{100}$$

$$\boldsymbol{\Phi}'_{1,0} = \boldsymbol{\Phi}_{1,0} \exp(\frac{1}{2}(k_{0,z}-k_{1,z})^2{\sigma_{0,1}}^2) \left(\frac{(k_{0,z}+k_{1,z})^2}{4k_{0,z}k_{1,z}} \exp(-(k_{0,z}-k_{1,z})^2{\sigma_{0,1}}^2) - \frac{(k_{0,z}-k_{1,z})^2}{4k_{0,z}k_{1,z}} \exp(-(k_{0,z}+k_{1,z})^2{\sigma_{0,1}}^2) \right) \tag{101}$$

The modified Fresnel refraction coefficients $\Phi'_{0,1}$ corresponds to equation (10.29) in p.200 of Holy[14], equation (8.24) in p.242 of Daillant [15] and equation (1.117) in p.29 of Sakurai [20]. However, no one obtained the expression corresponding to $\Phi'_{1,0}$. It is peculiar that $\Phi'_{1,0}$ and $\Phi'_{0,1}$ are asymmetrical. It comes to cause a different result if 1-th layer and 0-th layers are replaced and calculated. Therefore this derived Φ' should not be used to calculate the reflectivity from rough surfaces and interfaces.

The derived Fresnel refraction coefficients Φ' increase. This increase in the transmission coefficient completely overpowers any decrease in the value of the reflection coefficient as the following,

$$\boldsymbol{\Phi}'_{0,1}\boldsymbol{\Phi}'_{1,0} - \boldsymbol{\Psi}'_{0,1}\boldsymbol{\Psi}'_{1,0} = 1 \tag{102}$$

$$\boldsymbol{\Phi}'_{j-1,j}\boldsymbol{\Phi}'_{j,j-1} - \boldsymbol{\Phi}_{j-1,j}\boldsymbol{\Phi}_{j,j-1} = \boldsymbol{\Psi}^2{}_{j,j-1}\left(1 - \exp(-2k_{j,z}k_{j-1,z}\sigma_{j,j-1}^2)\right) > 0 , \tag{103}$$

Moreover, if the deformation modulus of $\Phi'_{1,0}$ is assumed to be $\Phi'_{0,1}$, the left side of equation (102) exceeds unity, and therefore equation (100) is obviously wrong.

In Nevot and Croce's treatment of the Parratt formalism for the reflectivity calculation including surface and interface roughness, [2] the relations of the Fresnel coefficients between reflection and transmission as Equations (63), (82) and (102) were not shown. Furthermore, the modification of the Fresnel coefficients according to Nevot and Croce has been used for only surface and interface reflection. However, the modification of the transmission coefficients has an important role when the roughness of the surface or interface is high, and the effect of diffuse scattering due to that roughness should not be ignored, as shown in equation (83). The error in Nevot and Croce's treatment [2] originates in the fact that the modified Fresnel coefficients was calculated based on the Parratt formalism which contains the x-ray energy conservation rule at the surface and interface. In the discussion on pp.767-768 of Nevot and Croce's [2], their Fresnel coefficients at the rough interface fulfil x-ray energy flow conservation at the interface, and so diffuse scattering was ignored at the rough interface. In their discussion, the transmission coefficients t_R and t_I were replaced approximately by the reflection coefficients r_R and r_I by the ignoring diffuse scattering term, and according to the principle of conservation energy. The reflection coefficient r_R at the rough interface should be expressed as a function of the reflection coefficient r_I and transmission coefficient t_I. However, the reflection coefficient r_R at the rough interface was expressed only by the reflection coefficient r_I, while the transmission coefficient t_I had already been replaced by the reflection coefficient r_I by the ignoring diffuse scattering term in the relationship based on the principle of the conservation of energy. Thus, the reflection coefficient r_R at

the rough interface as equation (11) of p.771 in Nevot and Croce [2] had been expressed with the reflection coefficient r_I only, and this results in the equation was also sure to include the conservation of energy.

The resulting increase in the transmission coefficient completely overpowers any decrease in the value of the reflection coefficient at the rough interface. Thus, because Nevot and Croce's treatment of the Parratt formalism contains a fundamental mistake regardless of the size of the roughness, results using this approach cannot be correct. The size of the modification of the transmission coefficient is one-order smaller than that of reflection coefficient, but, the size of transmission coefficient is one-order larger than the reflection coefficient at angles larger than critical angle. Thus, the errors of transmittance without the modification cannot be ignored.

Of course, there are cases where that Nevot and Croce's treatment can be applied. However, their method can be applied only to the case where there is no density distribution change at all in the direction parallel to the surface on the surface field side, and only when the scattering vector is normal to the surface. A typical example of surface medium to which this model can be applied is one where only the density distribution change in the vertical direction to the surface exists, as caused by diffusion etc. In such a special case, Nevot and Croce's treatment can be applied without any problem. However, because a general multilayer film always has structure in a direction parallel to the surface field side, Nevot and Croce's expression fails even when the roughness is extremely small. The use of only Fresnel reflection coefficients by Nevot and Croce is a fundamental mistake that does not depend on the size of the roughness.

2.5. The Refractive Fresnel Coefficient of a Rough Interface Used in New Reflectivity Calculations

To proceed, we therefore reconsider the derivation of the average value of the matrix as the same derivation of Eqs. (84), (85) when we consider the reduced Fresnel coefficient, which is known as the Croce-Nevot factor.

When the z position of the interface of the 0-th layer and 1-th layer $z_{o,1}$ fluctuates vertically as a function of the lateral position because of the interface roughness, the relations between the electric fields are derived by the use of the Fresnel coefficient tensor $\boldsymbol{\Phi}$ for refraction and the Fresnel coefficient tensor $\boldsymbol{\Psi}$ for reflection as follows

$$\begin{aligned} \boldsymbol{E}_1(z_{0,1}) &= \boldsymbol{\Phi}_{0,1}\boldsymbol{E}_0(z_{0,1}) + \boldsymbol{\Psi}_{1,0}\boldsymbol{E}'_1(z_{0,1}), \\ \boldsymbol{E}'_0(z_{0,1}) &= \boldsymbol{\Psi}_{0,1}\boldsymbol{E}_0(z_{0,1}) + \boldsymbol{\Phi}_{1,0}\boldsymbol{E}'_1(z_{0,1}), \end{aligned} \tag{104}$$

where

$$\begin{aligned} \boldsymbol{E}_0(z_{0,1}) &= \boldsymbol{E}_0(0)\exp[ik_{0,z}z_{0,1}], \quad \boldsymbol{E}'_0(0) = \boldsymbol{E}'_0(z_{0,1})\exp[ik_{0,z}z_{0,1}], \\ \boldsymbol{E}_1(z_{0,1}) &= \boldsymbol{E}_1(0)\exp[ik_{1,z}z_{0,1}], \quad \boldsymbol{E}'_1(0) = \boldsymbol{E}'_1(z_{0,1})\exp[ik_{1,z}z_{0,1}], \end{aligned} \tag{105}$$

then

$$\begin{aligned} \boldsymbol{E}_1(0)\exp[ik_{1,z}z_{0,1}] &= \boldsymbol{\Phi}_{0,1}\boldsymbol{E}_0(0)\exp[ik_{0,z}z_{0,1}] + \boldsymbol{\Psi}_{1,0}\boldsymbol{E}'_1(0)\exp[-ik_{1,z}z_{0,1}], \\ \boldsymbol{E}'_0(0)\exp[-ik_{0,z}z_{0,1}] &= \boldsymbol{\Psi}_{0,1}\boldsymbol{E}_0(0)\exp[ik_{0,z}z_{0,1}] + \boldsymbol{\Phi}_{1,0}\boldsymbol{E}'_1(0)\exp[-ik_{1,z}z_{0,1}]. \end{aligned} \tag{106}$$

Then the amplitudes A_0, A'_0, A_1, and A'_1 are derived as follows

$$\begin{aligned} \boldsymbol{A}_1\exp(ik_{1,z}z_{0,1}) &= \boldsymbol{\Phi}_{0,1}\boldsymbol{A}_0\exp(ik_{0,z}z_{0,1}) + \boldsymbol{\Psi}_{1,0}\boldsymbol{A}'_1\exp(-ik_{1,z}z_{0,1}), \\ \boldsymbol{A}'_0\exp(-ik_{0,z}z_{0,1}) &= \boldsymbol{\Psi}_{0,1}\boldsymbol{A}_0\exp(ik_{0,z}z_{0,1}) + \boldsymbol{\Phi}_{1,0}\boldsymbol{A}'_1\exp(-ik_{1,z}z_{0,1}). \end{aligned} \tag{107}$$

Matrix description of the relations is as follows,

$$\begin{pmatrix} \exp(-ik_{0,z}z_{0,1}) & 0 \\ 0 & \exp(ik_{1,z}z_{0,1}) \end{pmatrix}\begin{pmatrix} A'_0 \\ A_1 \end{pmatrix} = \begin{pmatrix} \boldsymbol{\Psi}_{0,1} & \boldsymbol{\Phi}_{1,0} \\ \boldsymbol{\Phi}_{0,1} & \boldsymbol{\Psi}_{1,0} \end{pmatrix}\begin{pmatrix} \exp(ik_{0,z}z_{0,1}) & 0 \\ 0 & \exp(-ik_{1,z}z_{0,1}) \end{pmatrix}\begin{pmatrix} A_0 \\ A'_1 \end{pmatrix} \tag{108}$$

$$\begin{pmatrix} A'_0 \\ A_1 \end{pmatrix} = \begin{pmatrix} \boldsymbol{\Psi}_{0,1}\exp(2ik_{0,z}z_{0,1}) & \boldsymbol{\Phi}_{1,0}\exp(-i(k_{1,z}-k_{0,z})z_{0,1}) \\ \boldsymbol{\Phi}_{0,1}\exp(i(k_{0,z}-k_{1,z})z_{0,1}) & \boldsymbol{\Psi}_{1,0}\exp(-2ik_{1,z}z_{0,1}) \end{pmatrix}\begin{pmatrix} A_0 \\ A'_1 \end{pmatrix} \tag{109}$$

then

$$\begin{pmatrix} A'_0 \\ A_1 \end{pmatrix} = \begin{pmatrix} \dfrac{k_{0,z}-k_{1,z}}{k_{0,z}+k_{1,z}}\exp(2ik_{0,z}z_{0,1}) & \dfrac{2k_{1,z}}{k_{0,z}+k_{1,z}}\exp(-i(k_{1,z}-k_{0,z})z_{0,1}) \\ \dfrac{2k_{0,z}}{k_{0,z}+k_{1,z}}\exp(i(k_{0,z}-k_{1,z})z_{0,1}) & \dfrac{k_{1,z}-k_{0,z}}{k_{0,z}+k_{1,z}}\exp(-2ik_{1,z}z_{0,1}) \end{pmatrix}\begin{pmatrix} A_0 \\ A'_1 \end{pmatrix} \tag{110}$$

We take the average value of this matrix.

$$\begin{pmatrix} A'_0 \\ A_1 \end{pmatrix} = \begin{pmatrix} \frac{k_{0,z}-k_{1,z}}{k_{0,z}+k_{1,z}}\left\langle \exp(2ik_{0,z}z_{0,1})\right\rangle & \frac{2k_{1,z}}{k_{0,z}+k_{1,z}}\left\langle \exp(-i(k_{1,z}-k_{0,z})z_{0,1})\right\rangle \\ \frac{2k_{0,z}}{k_{0,z}+k_{1,z}}\left\langle \exp(i(k_{0,z}-k_{1,z})z_{0,1})\right\rangle & \frac{k_{1,z}-k_{0,z}}{k_{0,z}+k_{1,z}}\left\langle \exp(-2ik_{1,z}z_{0,1})\right\rangle \end{pmatrix} \begin{pmatrix} A_0 \\ A'_1 \end{pmatrix} \tag{111}$$

For Gaussian statistics of standard deviation value σ,

$$\begin{pmatrix} A'_0 \\ A_1 \end{pmatrix} = \begin{pmatrix} \frac{k_{0,z}-k_{1,z}}{k_{0,z}+k_{1,z}}\exp(-2k^2{}_{0,z}\sigma_{0,1}{}^2) & \frac{2k_{1,z}}{k_{0,z}+k_{1,z}}\exp(-\frac{1}{2}(k_{0,z}-k_{1,z})^2\sigma_{0,1}{}^2) \\ \frac{2k_{0,z}}{k_{0,z}+k_{1,z}}\exp(-\frac{1}{2}(k_{0,z}-k_{1,z})^2\sigma_{0,1}{}^2) & \frac{k_{1,z}-k_{0,z}}{k_{0,z}+k_{1,z}}\exp(-2k^2{}_{1,z}\sigma_{0,1}{}^2) \end{pmatrix} \begin{pmatrix} A_0 \\ A'_1 \end{pmatrix} \tag{112}$$

then the Fresnel reflection coefficients Ψ' are found as follows

$$\Psi'_{0,1} = \Psi_{0,1}\exp(-2k^2{}_{0,z}\sigma_{0,1}^2),\ \ \Psi'_{1,0} = \Psi_{1,0}\exp(-2k^2{}_{1,z}\sigma_{0,1}^2). \tag{113}$$

and the Fresnel refraction coefficients Φ' are also produced similarly

$$\boldsymbol{\Phi}'_{0,1} = \boldsymbol{\Phi}_{0,1}\exp(-\frac{1}{2}(k_{0,z}-k_{1,z})^2\sigma_{0,1}{}^2) \qquad \boldsymbol{\Phi}'_{1,0} = \boldsymbol{\Phi}_{1,0}\exp(-\frac{1}{2}(k_{0,z}-k_{1,z})^2\sigma_{0,1}{}^2) \tag{114}$$

$$\boldsymbol{\Phi}'_{0,1}\boldsymbol{\Phi}'_{1,0} - \boldsymbol{\Psi}'_{0,1}\boldsymbol{\Psi}'_{1,0} = \frac{4k_{0,z}k_{1,z}}{(k_{0,z}+k_{1,z})^2}\exp(-(k_{0,z}-k_{1,z})^2\sigma_{0,1}{}^2) + (\frac{k_{1,z}-k_{0,z}}{k_{0,z}+k_{1,z}})^2\exp(-2(k^2{}_{0,z}+k^2{}_{1,z})\sigma_{0,1}{}^2) < 1 \tag{115}$$

The modified Fresnel refraction coefficients $\Phi'_{0,1}$ and $\Phi'_{1,0}$ of (114) corresponds to equation (1.115) on p.29 of Sakurai[20]. The Fresnel refraction coefficients Φ' derived by this method are reduced, and could be used to calculate the reflectivity from rough surface and interfaces. Accordingly, we calculated the reflectivity using these derived Fresnel refraction coefficients. However, the numerical results of this calculation did not agree with the experimental results when the angle of incidence smaller than the total reflection critical angle. In trying to account for the reason for this disagreement, it should be noticed that our present approach to constructing the reduced reflection coefficient $\Psi'_{0,1}$ term does not include any reference to the refractive index of the medium. Further, x-rays that penetrate an interface reflect from the interface below, and penetrate the former interface again without fail. Therefore, the refraction coefficient $\Phi'_{0,1}$ and $\Phi'_{1,0}$ should not be separately treated.

2.6. A New Formula for the Reflectivity for Rough Multilayer Surface

Once again we consider process by which we derive the average value of the matrix. When the z position of the interface of 0-th layer and 1-th layer $z_{o,1}$ fluctuates vertically as a function of the lateral position because of the interface roughness, the relations between the amplitudes A_0, A'_0, A_1, and A'_1 are shown by the use of the Fresnel coefficient tensor $\boldsymbol{\Phi}$ for refraction and the Fresnel coefficient tensor $\boldsymbol{\Psi}$ for reflection as follows

$$\begin{pmatrix} \exp(-ik_{0,z}z_{0,1}) & 0 \\ 0 & \exp(ik_{1,z}z_{0,1}) \end{pmatrix} \begin{pmatrix} A'_0 \\ A_1 \end{pmatrix} = \begin{pmatrix} \boldsymbol{\Psi}_{0,1} & \boldsymbol{\Phi}_{1,0} \\ \boldsymbol{\Phi}_{0,1} & \boldsymbol{\Psi}_{1,0} \end{pmatrix} \begin{pmatrix} \exp(ik_{0,z}z_{0,1}) & 0 \\ 0 & \exp(-ik_{1,z}z_{0,1}) \end{pmatrix} \begin{pmatrix} A_0 \\ A'_1 \end{pmatrix} \tag{116}$$

$$\begin{pmatrix} A'_0 \\ A_1 \end{pmatrix} = \frac{1}{\exp(-ik_{0,z}z_{0,1})\exp(ik_{1,z}z_{0,1})} \begin{pmatrix} \exp(ik_{1,z}z_{0,1}) & 0 \\ 0 & \exp(-ik_{0,z}z_{0,1}) \end{pmatrix} \begin{pmatrix} \boldsymbol{\Psi}_{0,1} & \boldsymbol{\Phi}_{1,0} \\ \boldsymbol{\Phi}_{0,1} & \boldsymbol{\Psi}_{1,0} \end{pmatrix} \begin{pmatrix} \exp(ik_{0,z}z_{0,1}) & 0 \\ 0 & \exp(-ik_{1,z}z_{0,1}) \end{pmatrix} \begin{pmatrix} A_0 \\ A'_1 \end{pmatrix} \tag{117}$$

$$\begin{pmatrix} A'_0 \\ A_1 \end{pmatrix} = \frac{1}{\exp(-ik_{0,z}z_{0,1})\exp(ik_{1,z}z_{0,1})} \begin{pmatrix} \exp(ik_{1,z}z_{0,1})\boldsymbol{\Psi}_{0,1}\exp(ik_{0,z}z_{0,1}) & \exp(ik_{1,z}z_{0,1})\boldsymbol{\Phi}_{1,0}\exp(-ik_{1,z}z_{0,1}) \\ \exp(-ik_{0,z}z_{0,1})\boldsymbol{\Phi}_{0,1}\exp(ik_{0,z}z_{0,1}) & \exp(-ik_{0,z}z_{0,1})\boldsymbol{\Psi}_{1,0}\exp(-ik_{1,z}z_{0,1}) \end{pmatrix} \begin{pmatrix} A_0 \\ A'_1 \end{pmatrix} \tag{118}$$

$$\begin{pmatrix} A'_0 \\ A_1 \end{pmatrix} = \frac{1}{\exp(-ik_{0,z}z_{0,1})\exp(ik_{1,z}z_{0,1})} \begin{pmatrix} \boldsymbol{\Psi}_{0,1}\exp(i(k_{1,z}+k_{0,z})z_{0,1}) & \boldsymbol{\Phi}_{1,0}\exp(i(k_{1,z}-k_{1,z})z_{0,1}) \\ \boldsymbol{\Phi}_{0,1}\exp(i(-k_{0,z}+k_{0,z})z_{0,1}) & \boldsymbol{\Psi}_{1,0}\exp(i(-k_{0,z}-k_{1,z})z_{0,1}) \end{pmatrix} \begin{pmatrix} A_0 \\ A'_1 \end{pmatrix} \tag{119}$$

$$\begin{pmatrix} A'_0 \\ A_1 \end{pmatrix} = \begin{pmatrix} \boldsymbol{\Psi}_{0,1} \dfrac{\exp(i(k_{1,z}+k_{0,z})z_{0,1})}{\exp(i(-k_{0,z}+k_{1,z})z_{0,1})} & \boldsymbol{\Phi}_{1,0}\exp(i(k_{0,z}-k_{1,z})z_{0,1}) \\ \boldsymbol{\Phi}_{0,1}\exp(i(-k_{1,z}+k_{0,z})z_{0,1}) & \boldsymbol{\Psi}_{1,0} \dfrac{\exp(i(-k_{0,z}-k_{1,z})z_{0,1})}{\exp(i(-k_{0,z}+k_{1,z})z_{0,1})} \end{pmatrix} \begin{pmatrix} A_0 \\ A'_1 \end{pmatrix} \tag{120}$$

Again, we take the average value of this matrix,

$$\begin{pmatrix} A'_0 \\ A_1 \end{pmatrix} = \begin{pmatrix} \boldsymbol{\Psi}_{0,1} \dfrac{\langle \exp(i(k_{1,z}+k_{0,z})z_{0,1})\rangle}{\langle \exp(i(-k_{0,z}+k_{1,z})z_{0,1})\rangle} & \boldsymbol{\Phi}_{1,0}\langle \exp(i(k_{0,z}-k_{1,z})z_{0,1})\rangle \\ \boldsymbol{\Phi}_{0,1}\langle \exp(i(-k_{1,z}+k_{0,z})z_{0,1})\rangle & \boldsymbol{\Psi}_{1,0} \dfrac{\langle \exp(i(-k_{0,z}-k_{1,z})z_{0,1})\rangle}{\langle \exp(i(-k_{0,z}+k_{1,z})z_{0,1})\rangle} \end{pmatrix} \begin{pmatrix} A_0 \\ A'_1 \end{pmatrix} \tag{121}$$

For Gaussian statistics of standard deviation value σ, the Fresnel reflection coefficient $\boldsymbol{\Psi}'$ are as follows

$$\boldsymbol{\Psi}'_{0,1} = \boldsymbol{\Psi}_{0,1} \frac{\langle \exp(i(k_{1,z}+k_{0,z})z_{0,1})\rangle}{\langle \exp(i(-k_{0,z}+k_{1,z})z_{0,1})\rangle} = \boldsymbol{\Psi}_{0,1} \frac{\exp(-\frac{1}{2}(k_{0,z}+k_{1,z})^2\sigma_{0,1}{}^2)}{\exp(-\frac{1}{2}(k_{0,z}-k_{1,z})^2\sigma_{0,1}{}^2)} = \boldsymbol{\Psi}_{0,1}\exp(-2k_{0,z}k_{1,z}\sigma_{0,1}{}^2). \tag{122}$$

$$\boldsymbol{\Psi}'_{1,0} = \boldsymbol{\Psi}_{1,0} \frac{\langle \exp(i(-k_{0,z}-k_{1,z})z_{0,1})\rangle}{\langle \exp(i(-k_{0,z}+k_{1,z})z_{0,1})\rangle} = \boldsymbol{\Psi}_{1,0} \frac{\exp(-\frac{1}{2}(-k_{0,z}-k_{1,z})^2\sigma_{0,1}{}^2)}{\exp(-\frac{1}{2}(k_{1,z}-k_{0,z})^2\sigma_{0,1}{}^2)} = \boldsymbol{\Psi}_{1,0}\exp(-2k_{0,z}k_{1,z}\sigma_{0,1}{}^2). \tag{123}$$

Because x-rays that penetrate an interface reflect from the interface below, and penetrate former interface again without fail, it is necessary to treat the refraction coefficients $\boldsymbol{\Phi}'_{0,1}$ and $\boldsymbol{\Phi}'_{1,0}$ collectively.

$$\begin{aligned} \boldsymbol{\Phi}'_{0,1}\boldsymbol{\Phi}'_{1,0} &= \langle \boldsymbol{\Phi}_{0,1}\exp(i(-k_{1,z}+k_{0,z})z_{0,1})\boldsymbol{\Phi}_{1,0}\exp(i(k_{0,z}-k_{1,z})z_{0,1})\rangle \\ &= \boldsymbol{\Phi}_{0,1}\boldsymbol{\Phi}_{1,0}\langle \exp(i(-k_{1,z}+k_{0,z})z_{0,1})\exp(i(k_{0,z}-k_{1,z})z_{0,1})\rangle \\ &= \boldsymbol{\Phi}_{0,1}\boldsymbol{\Phi}_{1,0}\langle \exp(i(2k_{0,z}-2k_{1,z})z_{0,1})\rangle \\ &= \boldsymbol{\Phi}_{0,1}\boldsymbol{\Phi}_{1,0}\exp(-2(k_{0,z}-k_{1,z})^2\sigma_{0,1}{}^2) \end{aligned} \tag{124}$$

Then the Fresnel coefficients $\boldsymbol{\Psi}'$ and $\boldsymbol{\Phi}'$ are reduced as follows

$$\boldsymbol{\Psi}'_{0,1} = \boldsymbol{\Psi}_{0,1}\exp(-2k_{0,z}k_{1,z}\sigma_{0,1}^2), \quad \boldsymbol{\Psi}'_{1,0} = \boldsymbol{\Psi}_{1,0}\exp(-2k_{0,z}k_{1,z}\sigma_{0,1}^2),$$

$$\boldsymbol{\Phi}'_{0,1} = \boldsymbol{\Phi}_{0,1}\exp(-(k_{0,z}-k_{1,z})^2\sigma_{0,1}{}^2), \quad \boldsymbol{\Phi}'_{1,0} = \boldsymbol{\Phi}_{1,0}\exp(-(k_{0,z}-k_{1,z})^2\sigma_{0,1}{}^2), \tag{125}$$

$$\begin{pmatrix} A'_0 \\ A_1 \end{pmatrix} = \begin{pmatrix} \boldsymbol{\Psi}'_{0,1} & \boldsymbol{\Phi}'_{1,0} \\ \boldsymbol{\Phi}'_{0,1} & \boldsymbol{\Psi}'_{1,0} \end{pmatrix} \begin{pmatrix} A_0 \\ A'_1 \end{pmatrix} \tag{126}$$

Then

$$\begin{pmatrix} A'_0 \\ A_1 \end{pmatrix} = \begin{pmatrix} \boldsymbol{\Psi}_{0,1}\exp(-2k_{0,z}k_{1,z}\sigma_{0,1}{}^2) & \boldsymbol{\Phi}_{1,0}\exp(-(k_{0,z}-k_{1,z})^2\sigma_{0,1}{}^2) \\ \boldsymbol{\Phi}_{0,1}\exp(-(k_{0,z}-k_{1,z})^2\sigma_{0,1}{}^2) & \boldsymbol{\Psi}_{1,0}\exp(-2k_{0,z}k_{1,z}\sigma_{0,1}{}^2) \end{pmatrix} \begin{pmatrix} A_0 \\ A'_1 \end{pmatrix} \tag{127}$$

$$\begin{pmatrix} A'_0 \\ A_1 \end{pmatrix} = \begin{pmatrix} \dfrac{k_{0,z}-k_{1,z}}{k_{0,z}+k_{1,z}}\exp(-2k_{0,z}k_{1,z}\sigma_{0,1}{}^2) & \dfrac{2k_{1,z}}{k_{0,z}+k_{1,z}}\exp(-(k_{0,z}-k_{1,z})^2\sigma_{0,1}{}^2) \\ \dfrac{2k_{0,z}}{k_{0,z}+k_{1,z}}\exp(-(k_{0,z}-k_{1,z})^2\sigma_{0,1}{}^2) & \dfrac{k_{1,z}-k_{0,z}}{k_{0,z}+k_{1,z}}\exp(-2k_{0,z}k_{1,z}\sigma_{0,1}{}^2) \end{pmatrix} \begin{pmatrix} A_0 \\ A'_1 \end{pmatrix} \tag{128}$$

and

$$\boldsymbol{\Phi}'_{0,1}\boldsymbol{\Phi}'_{1,0}-\boldsymbol{\Psi}'_{0,1}\boldsymbol{\Psi}'_{1,0}=\frac{4k_{0,z}k_{1,z}}{(k_{0,z}+k_{1,z})^2}\exp(-2(k_{0,z}-k_{1,z})^2\sigma_{0,1}{}^2)+(\frac{k_{1,z}-k_{0,z}}{k_{0,z}+k_{1,z}})^2\exp(-4k_{0,z}k_{1,z}\sigma_{0,1}{}^2)<1 \quad (129)$$

The Fresnel refraction coefficients $\boldsymbol{\Phi}'$ derived by this method are reduced, and can be used to calculate the reflectivity from rough surface and interface. Therefore, we calculate the reflectivity using these newly-derived Fresnel coefficients in an accurate reflectivity equation of $R_{j\text{-}1,j}$ and $R_{j,j+1}$ as follows,

$$\boldsymbol{R}_{j-1,j}=\frac{\boldsymbol{\Psi}'_{j-1,j}+(\boldsymbol{\Phi}'_{j-1,j}\boldsymbol{\Phi}'_{j,j-1}-\boldsymbol{\Psi}'_{j-1,j}\boldsymbol{\Psi}'_{j,j-1})\boldsymbol{R}_{j,j+1}}{1-\boldsymbol{\Psi}'_{j,j-1}\boldsymbol{R}_{j,j+1}}\exp(2ik_{j-1,z}h_{j-1}), \quad (130)$$

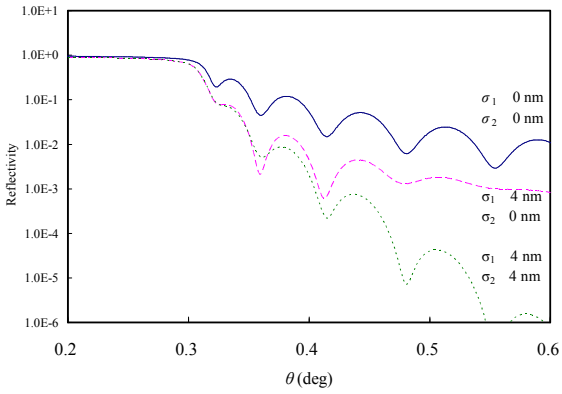

Figure 6. *New calculated reflectivities from a GaAs layer with a thickness of 48 nm on a Si substrate. The line is for a flat surface and a flat interface. The dashed curve is for a surface roughness σ_1 of 4 nm and with a flat interface, while the dotted curve is for a surface roughness σ_1 of 4 nm and interface roughness σ_2 of 4 nm.*

Based on the above considerations, we again calculated the x-ray reflectivity for the GaAs/Si system, but now considered the effect of attenuation in the refracted x-rays by diffuse scattering resulting from surface roughness. The results are shown as the dashed line in Figure 6 for a surface roughness of 4 nm and flat interface, and the dotted line shows the calculated result in the case that the surface and interface both have a rms roughness of 4 nm.

The ratio of the oscillation amplitude to the size of the reflectivity in the reflectivity curve (dot) in Figure 6 is smaller than that of the reflectivity curve Figure 3. In the reflectivity curve (dashed line), the very large amplitude of the oscillation near an angle of incidence of 0.36° in Figure 3 has disappeared in Figure 6. These results are now physically reasonable. All the strange results seen in Figure 3 have disappeared in Figure 6. It seems natural that the effect of interference does decrease at a rough surface and interface, because the amount of coherent x-rays should reduce due to diffuse scattering.

Figure 7 shows the new calculated reflectivity for surface roughnesses of 3.5 nm, 4 nm, and 4.5 nm, and with a flat interface. At all angles of incidence, the reflectivity of the surface roughness of 4 nm is near the mean value of the reflectivity of the surface roughness of 3.5 nm and the reflectivity of the surface roughness of 4.5 nm. This result is physically reasonable, because the value of the roughness is the standard deviation value of various amplitudes of rough surface. However, it was difficult to match the numerical result of x-ray reflectivity to the results of TEM observation.

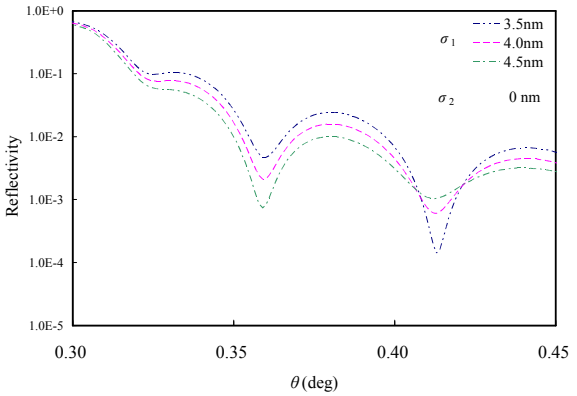

Figure 7. *New calculated reflectivity from a GaAs layer with a thickness of 48 nm on a Si substrate. In the calculation, the interface roughness σ_2 is 0 nm. Three calculated results for a GaAs surface with roughness σ_1 of 3.5 nm, 4 nm, and 4.5 nm are shown.*

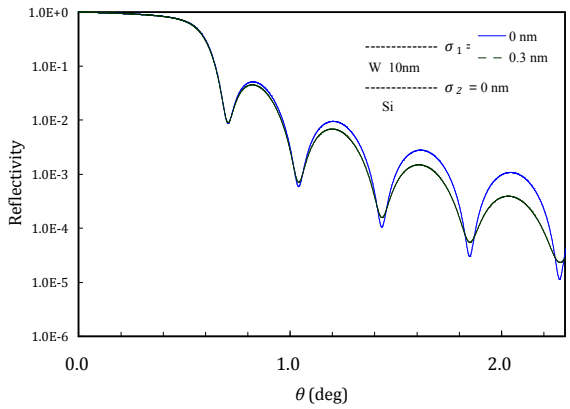

Figure 8. *X-ray reflectivity from a silicon wafer covered with a thin (10 nm) tungsten film calculated by the new calculation that considered diffuse scattering. Solid line shows the case of a flat surface. Dashed line shows the case of a surface with a rms surface roughness of 0.3 nm.*

Next, we again calculated the X-ray reflectivity for the W/Si system, but now considered the effect of attenuation in the refracted X rays by diffuse scattering resulting from surface roughness. However, the reduced refraction coefficient in prior work varies. [14-18, 20-23] Then about the reduced refraction coefficient, reduction as same as reflection coefficient was applied now. Figure 8 shows the calculated results with the use of improved X-ray reflectivity formalism. In the reflectivity curve from a surface with an rms surface roughness of 0.3 nm (dashed line), the amplitude of the

oscillation in Figure 5 has reduced in Figure 8. These results are now physically reasonable. The strange results seen in Figure 5 have disappeared in Figure 8. It seems natural that the effect of interference does decrease at a rough surface and interface, because the amount of coherent X rays should reduce due to diffuse scattering.

3. TEM Observation and X-ray Reflectivity Measurement for Surfaces and Interfaces of Multilayered Thin Film Materials

The surface and interfacial roughness of the same sample of multilayered thin film material was measured by transmission electron microscopy (TEM) and compared them with those from x-ray reflectivity measurements. The surface sample for examination was prepared as follows; a GaAs layer was grown on Si(110) by molecular beam epitaxy (MBE). From TEM observations, the thickness of the GaAs layer was 48 nm, the root-mean-square (rms) roughness of the GaAs surface was about 2.8 nm, the rms roughness of the interface between GaAs and Si was about 0.7 nm. Figure 9 shows a cross section image of this GaAs / Si(110) sample observed by TEM.

X-ray reflectivity measurements were performed using a Cu-Kα x-ray beam from an 18 kW rotating-anode source. Figure 10 shows the measured reflectivity of x-rays (wave length 0.154 nm) from a GaAs layer with a thickness of 48 nm on a silicon wafer. The decrease in signal for angles larger than the total reflection critical angle shows oscillations. These oscillations are caused by interference between x-rays that reflect from the surface of GaAs layer and those that reflect from the interface of the GaAs layer and Si substrate. The characteristics of these oscillations reflect the surface roughness and the interface roughness. The angular resolution in the measurement was 0.002 degree. This resolution is adequately smaller than oscillation period (about 0.04°) of XRR. Then we compared the measurement data with calculation without fitting correction.

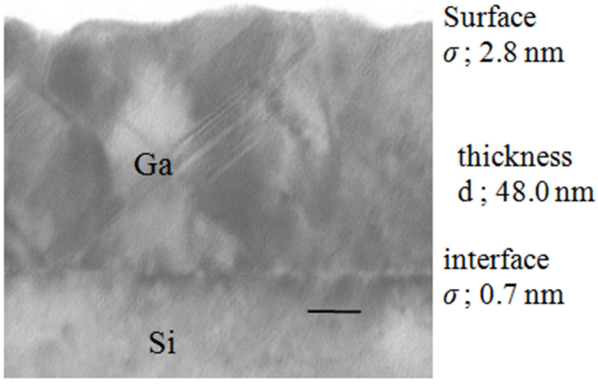

Figure 9. *Cross section image of GaAs / Si(110) by TEM observation.*

At the first, we simulated the XRR data by conventional XRR formalism shown as,

$$\Psi'_{j-1,j} = \frac{k_{j-1,z} - k_{j,z}}{k_{j-1,z} + k_{j,z}} \exp\left(-2k_{j-1,z}k_{j,z}\sigma_{j-1,j}^{\,2}\right), \quad \Psi'_{j,j-1} = -\Psi'_{j-1,j}$$

$$R = \left|R_{0,1}\right|^2, \quad R_{j-1,j} = \frac{\Psi'_{j-1,j} + R_{j,j+1}}{1 - \Psi'_{j,j-1}R_{j,j+1}} \exp(2ik_{j-1,z}h_{j-1}), \quad R_{N,N+1} = 0$$

Figure 11 shows the result (dots) of a calculation based on these expressions of the reflectivity of x-rays from a GaAs layer with a thickness of 48 nm on Si substrate. The rms roughness of the interface of GaAs and Si was set to 0.7 nm, the value derived from the TEM observations. The rms roughness of the GaAs surface was set to 2.8 nm, the value derived from the AFM measurements. The agreement of the calculated and experimental results in Figure 2 is not good.

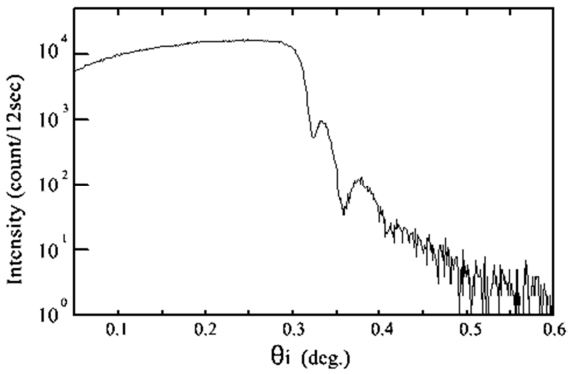

Figure 10. *Measured x-ray reflectivity from a silicon wafer covered with a thin (48 nm) GaAs layer.*

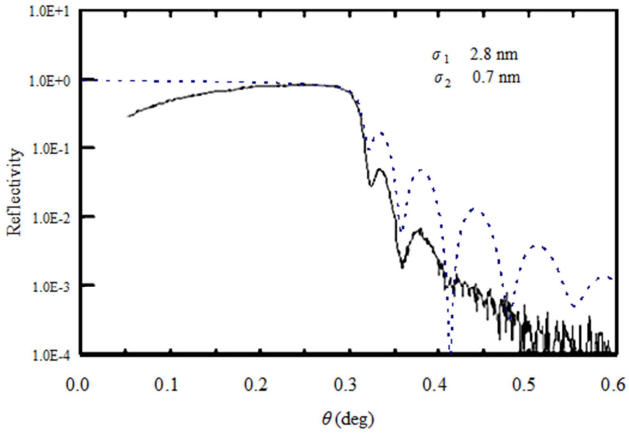

Figure 11. *Calculated (dots) and measured (line) reflectivity from a GaAs layer with a thickness of 48 nm on a Si substrate. The surface roughness σ_1 is 2.8 nm and the interfacial roughness σ_2 is 0.7 nm.*

The calculated result suggests the following: if the value of the surface roughness and the interfacial roughness in the calculation would be made larger, the calculated result will more closely approach the experimental result. In the TEM observation and AFM measurements, one half of the peak to peak value of the interface roughness equates to 1 nm, and that of the GaAs surface is 4 nm. We then recalculated the reflectivity values of this order for the surface roughness and the interface roughness in the calculation. Three calculated

results for a roughness of GaAs surface of 3.5 nm, 4 nm, and 4.5 nm, with an interface roughness of 1 nm are shown in Figure 12.

Although the calculated results did more closely approach those from experiment, they still showed poor agreement. The ratio of the oscillation amplitude to the value of the reflectivity near an angle of incidence of 0.36° in the calculated reflectivity for the GaAs surface of 4 nm roughness in Figure 12 is larger than that of the reflectivity for a small roughness of 2.8 nm in Figure 11, *i. e.*, near an angle of incidence of 0.36° interference effects appear to increase the reflectivity in the case of large roughness. It seems very strange that interference effects would operate in this way.

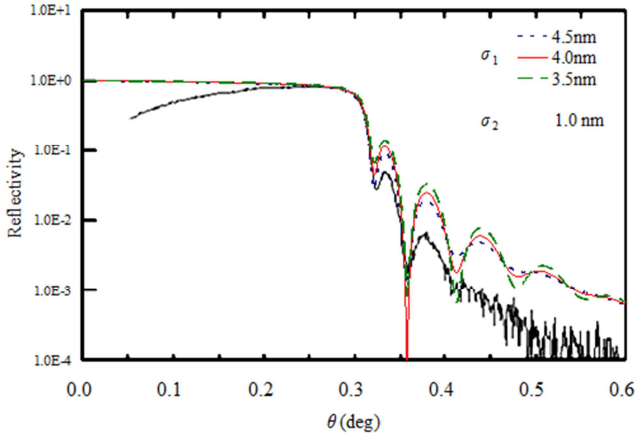

Figure 12. *Calculated (dotted, dashed and thin lines) and measured (thick line) reflectivity from a GaAs layer with a thickness of 48 nm on a Si substrate. In the calculation, the interface roughness σ_2 is 1.0 nm. Three calculated results with the roughness σ_1 of GaAs surface set at 3.5 nm, 4 nm, and 4.5 nm, are shown.*

This disagreement was mainly caused by the fact that the diffuse scattering at the rough interface was not correctly taken into account by Nevot and Croce [2]. For reproducing the result of measurement XRR, the calculated interfacial roughness σ_2 should not be 0.7 nm in conventional XRR formalism of Eq. 58. The result of interfacial roughness by the conventional XRR formulae showed large difference with the TEM result, and derived wrong structure of surface.

Next, we show applying of new improved formalism for this result of XRR measurement with a TEM observation. Then, in the calculation of XRR when there is roughening at the surface or the interface, the Fresnel transmission coefficient $\Phi'_{j-1,j}$ should be used for the reduced coefficient. Although formula for $\Psi_{j-1,j}$ is well known

$$\Psi_{j-1,j} = \frac{k_{j-1,z} - k_{j,z}}{k_{j-1,z} + k_{j,z}} \exp\left(-2k_{j-1,z}k_{j,z}\sigma_{j-1,j}^{\ 2}\right), \quad \Psi_{j,j-1} = -\Psi_{j-1,j}, \tag{131}$$

an accurate analytical formula for $\Phi_{j-1,j}$ including the effect of the interface roughness is not available. Several theories exist to describe the influence of roughness on X-ray scattering, and the Fresnel coefficient for transmission has been derived in several theories. [14-18, 20-23] There are several approximations proposed so far and all these results can be written by including any parameters depend on the proposed approximations as

$$\begin{aligned} \boldsymbol{\Phi}_{j-1,j} &= \frac{2\boldsymbol{k}_{j-1,z}}{\boldsymbol{k}_{j-1,z} + \boldsymbol{k}_{j,z}} \exp\{-[\boldsymbol{C}_1(\boldsymbol{k}_{j-1,z} - \boldsymbol{k}_{j,z})^2 + \boldsymbol{C}_2\boldsymbol{k}_{j-1,z}\boldsymbol{k}_{j,z}]\boldsymbol{\sigma}_{0,1}^{\ 2}\}, \\ \boldsymbol{\Phi}_{j,j-1} &= \boldsymbol{\Phi}_{j-1,j}\frac{\boldsymbol{k}_{j,z}}{\boldsymbol{k}_{j-1,z}} \end{aligned} \tag{132}$$

where parameters C_1, C_2 depend on the proposed approximation. [14-18, 20-23] With the use of the reduced Fresnel reflection coefficient $\Psi'_{j-1,j}$ of Eq. (3) and the reduced Fresnel transmission coefficient $\Phi'_{j-1,j}$ of Eq. (10), new accurate reflectivity R from a multilayer consisting of N layers with rough surface and interfaces is shown as

$$\begin{aligned} R &= \left|R_{0,1}\right|^2, \\ R_{j-1,j} &= \frac{\Psi_{j-1,j} + (\Phi_{j-1,j}\Phi_{j,j-1} - \Psi_{j-1,j}\Psi_{j,j-1})R_{j,j+1}}{1 - \Psi_{j,j-1}R_{j,j+1}} \exp(2ik_{j-1,z}h_{j-1}), \\ R_{N,N+1} &= 0 \end{aligned} \tag{133}$$

In the previous analysis, the reduction of transmission coefficient has not be examined by the other experiment. Then in this study, we tried to determine the parameters C_1, C_2 in Eq. (11) experimentally by comparing the measurements of TEM observation results and XRR. The XRR from a GaAs layer with a thickness of 48 nm on Si substrate, where surface roughness σ_s was set to 5.5 nm and interface roughness σ_i was set to 0.7 nm, was calculated with various C_1 and C_2. After choosing the parameters C_1, C_2 so that the calculation result of XRR accorded with the experimental result in this GaAs layer structure, $C_1 = 0$ and $C_2 = 0.2$ were provided. In Fig. 13, the dashed line shows the calculation result of XRR. The calculation results reproduce the experimental results almost well. As such, we could examine the physically reasonable reduction of transmission coefficient.

In the previous analysis, when it was supposed that σ_1 was 4.3 nm and σ_2 was 0.7 nm in this XRR measurement data [37], different parameters $C_1 = 0.5$ and $C_2 = 0.5$ were provided although the agreement of the calculation result and the experimental result was not more good than this time result. This suggests that the experimental XRR result can be reproduced almost well if appropriate parameters are chosen for different structure, like as even using conventional XRR formalism. Now we have got the parameters $C_1 = 0$ and $C_2 = 0.2$, but do not get physical grounds of the value of the parameters. It is thought that the value of the parameter C_1, C_2 depends on the structure of a parallel direction on the surface in the surface roughness and the interface roughness. Therefore, the investigation about many samples will be necessary in future.

The result of interfacial roughness by using the conventional XRR formulae showed large difference with the TEM result, and derived wrong structure of surface. While, the result by new improved formalism reproduce the TEM result, but need appropriate parameters in transmission coefficient. It shows that new improved XRR formalism derives more accurate analysis of the XRR from a multilayer

surface, but the reduced Fresnel coefficients with physical grounds in the reflectivity equation are need in further research and we continue to discuss the refining this theory in next section.

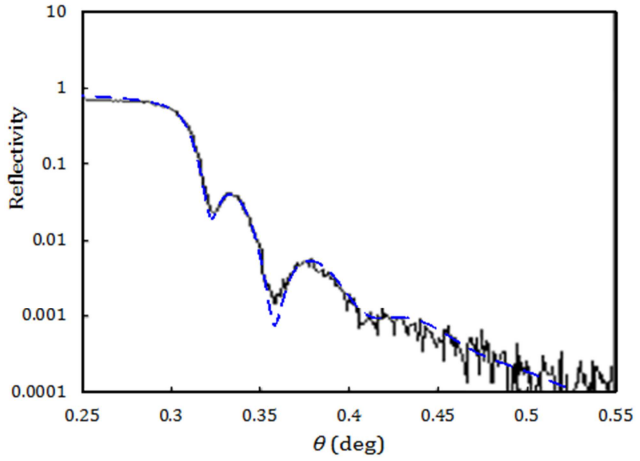

Figure 13. *Solid line shows measured XRR from a GaAs layer with a thickness of 48 nm on a Si substrate. Dashed line shows calculated reflectivity by improved formalism with the parameters $C_1 = 0$, $C_2 = 0.2$ for reproducing measurement XRR when σ_1 is 5.5 nm and σ_2 is 0.7 nm.*

4. Surface and Interface Roughness Estimations by X-ray Reflectivity with AFM Observation and RBS Measurements

For deriving more accurate formalism of x-ray reflectivity, combination of XRR with other analytical techniques could be useful. We tried to compare the measurements of the surface roughness of the same sample by x-ray reflectivity (XRR) with atomic force microscopy (AFM) and high-resolution Rutherford backscattering spectroscopy (HRBS). XRR is generally less sensitive to the interface roughness σ_i compared with the surface roughness σ_s. AFM is widely used to measure the surface structures, and HRBS is widely used to measure the interface structures [42]. Although HRBS cannot directly measure the interface roughness it can measure the film thickness and its dispersion σ_t. With the help of the HRBS measurement, XRR can provide more accurate estimate of the interface roughness σ_i.

4.1. Sample Preparation

Two samples of silicon wafers having a thin SiO_2 layer were prepared by the following methods. The sample A was prepared by thermal oxidizing of a Si(001) wafer. The thickness of the prepared SiO_2 layer is about 5 nm. The other sample B was prepared by vacuum deposition of an additional SiO_2 layer of about 2 nm on the sample A at room temperature. The roughness of the SiO_2/Si interface is expected to be the same as the sample A although the surface roughness should be increased after the deposition. The surface and interface roughnesses of these samples were measured by XRR, AFM and HRBS.

4.2. AFM Observation

The surfaces of sample A and sample B were observed by atomic force microscopy (AFM). Figure 14 show the AFM images and the roughness profiles of sample A and sample B, respectively. The r.m.s. roughness σ_s at the area of 1×1 μm^2 of the SiO_2 surfaces of sample A and sample B in Figures 14 (a) - (b) were about 0.17 nm both, and those at the area of 10×10 μm^2 in Figures 14 (c) - (d) were about 0.24 nm both. AFM observation shows that the surface roughness was hardly a change before and after vapor deposition of the SiO_2.

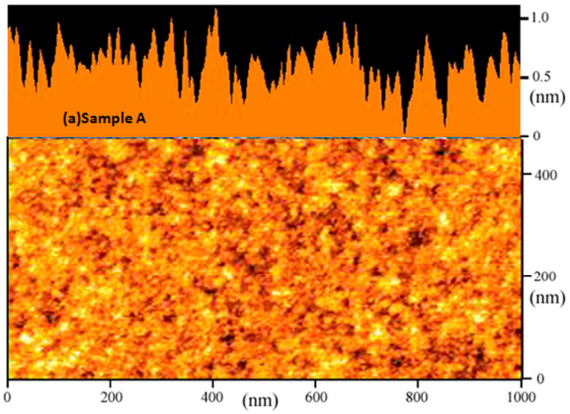

Fig. 14(a). *The AFM images and the roughness profiles of sample A (in the area of 1μm square).*

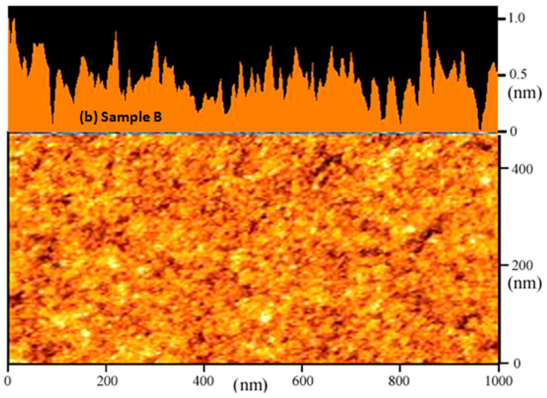

Fig. 14(b). *The AFM images and the roughness profiles of sample B (in the area of 1μm square).*

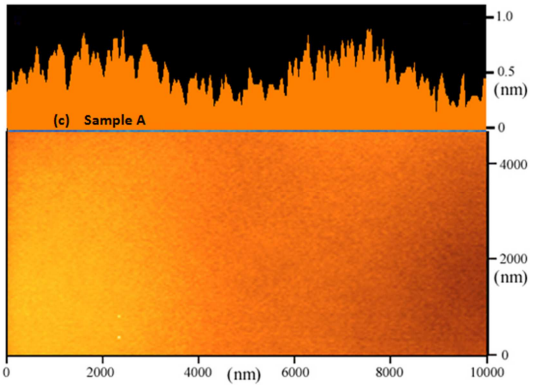

Fig. 14(c). *The AFM images and the roughness profiles of sample A (in the area of 10 μm square).*

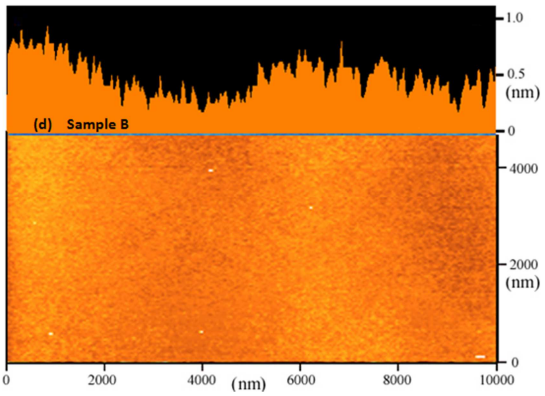

Fig. 14(d). The AFM images and the roughness profiles of sample B (in the area of 10 μm square).

4.3. HRBS Measurement

The details of the HRBS measurement were described elsewhere [43, 44]. Briefly, a beam of 400-keV He^+ ions from a Cockcroft Walton type accelerator was collimated to 2 × 2 mm^2 and to a divergence angle of less than 0.1° by a series of 4-jaw slit systems. The well-collimated beam was transported to an ultra-high-vacuum (UHV) scattering chamber (base pressure 1 × 10^{-8} Pa) via a differential pumping system and impinged on a target mounted on a 5-axis precision goniometer. The typical beam current was about 30 nA. The He^+ ions scattered from the target at a scattering angle $\theta \approx 50°$ were energy analyzed by a 90° sector type magnetic spectrometer and detected by a one-dimensional position sensitive detector (1D-PSD) of 100 mm length (the energy window was 25% of the central energy). The energy resolution of the spectrometer was ~ 0.1%. The surface of the sample was cleaned using the ultraviolet/ozone cleaning method before the HRBS measurement.

Figure 15 shows the HRBS spectra observed at a scattering angle of 50.3°, when 400 keV He^+ ions were incident on the sample A. In addition to a random spectrum (triangles), the [111] channeling spectrum (circles) was also measured to observe the surface and interface structures more precisely. The angle of incidence of He^+ ions was 54.9° and 50.4° (exit angles were θ_e = 74.8° and 79.3°) for the channeling and the random spectra, respectively. In the channeling spectrum, there are two trapezoidal structures at ~ 355 keV and ~ 330 keV. These structures correspond to the silicon and oxygen signals in the SiO_2 layer. The width of the oxygen signal is 9.29 keV, which corresponds to a SiO_2 layer of 5.2 nm. The surface and interface edges (seen at ~ 333 and 325 keV, respectively) of the oxygen signal were fitted by error functions as is shown by solid curves. The standard deviation, Ω_s, of the error function for the surface edge was determined to be 0.47 keV, which is ascribed to the instrumental energy resolution including the energy spread of the incident beam. On the other hand, the standard deviation, Ω_i, for the interface edge was 1.62 keV, which includes effects of the energy loss straggling and the non-uniformity of the SiO_2 layer.

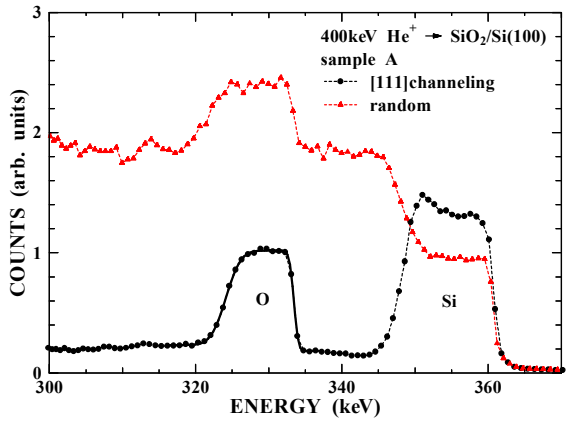

Fig. 15. HRBS spectra of sample A. The [111] channeling and the random spectra are shown by circles and triangles, respectively.

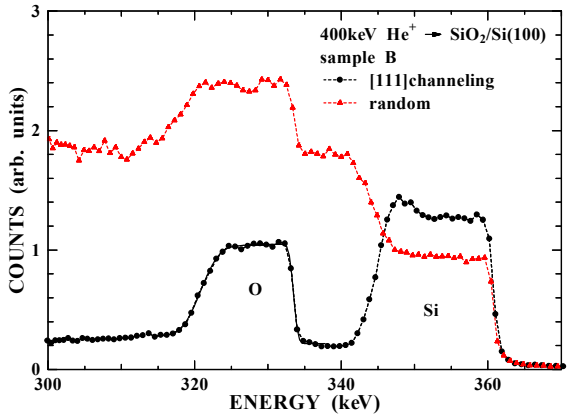

Fig. 16. HRBS spectra of sample B. The [111] channeling and the random spectra are shown by circles and triangles, respectively.

Figure 16 shows the [111] channeling and random spectra of the sample B. The angles of incidence of He^+ ions were 54.4° and 49.9° (exit angles were θ_e = 75.3° and 79.8°) for the [111] channeling and the random spectra, respectively. The width of the oxygen signal in the channeling spectrum was 12.6 keV, which corresponds to a SiO_2 layer of 7.4 nm. The leading and trailing edges of the oxygen signal in the channeling spectrum were fitted by error functions as is shown by solid curves. The standard deviation of the surface edge was determined to be 0.47 keV, showing a good agreement with the sample A. The standard deviation of the interface edge was determined to be 2.01 keV. This is larger than that of the sample A, indicating that the non-uniformity of the SiO_2 layer is increased by the deposition of SiO_2.

The observed Ω_i is affected by the instrumental energy resolution, which is given by the observed Ω_s, and also affected by the energy loss straggling. The effect of the energy loss straggling, Ω_{str}, was calculated using the empirical formula given by Yang et al [45]. The calculated results are 1.05 and 1.25 keV for the sample A and B, respectively. The non-uniformity of the SiO_2 layer is estimated by $\Omega_t^2 = \Omega_i^2 - \Omega_{str}^2 - \Omega_s^2$. The obtained results are Ω_t = 1.14 keV and 1.5 keV for sample A and B, respectively. Using the stopping power of SiO_2, the dispersion σ_t of the SiO_2 layer thickness was derived as 0.67 nm and 0.88 nm for

the sample A and B, respectively. The difference between the sample A and B is attributed to the increase of the surface roughness due to the deposition of 2-nm SiO_2 layer.

4.4. X-ray Reflectivity Measurement

X-ray reflectivity measurements were performed using a Cu-Kα x-ray beam from a 3 kW rotating-anode source. The beam size of the x-ray was about 2 mm (perpendicular to the reflection plane) × 0.05 mm (parallel to the reflection plane). The results of the x-ray reflectivity measured for the sample A and B are shown as a function of the angle of incidence, θ_i, by dashed curves in Figs. 17 and 18, respectively. At θ_i smaller than the critical angle for total reflection (0.22°), the reflectivity is almost unity. With increasing θ_i over the critical angle, the reflectivity decreases and oscillatory structures are seen. These oscillations originate from the interference of x-rays reflected from the surface and the interface of the SiO_2/Si. By analysing the θ_i–dependence of the reflectivity, the surface roughness, interface roughness and the thickness of the SiO_2 layer can be estimated.

Now, we show applying of the following new improved formalism for this result of XRR measurement.

$$R = \left|R_{0,1}\right|^2 ,$$

$$R_{j-1,j} = \frac{\Psi_{j-1,j} + (\Phi_{j-1,j}\Phi_{j,j-1} - \Psi_{j-1,j}\Psi_{j,j-1})R_{j,j+1}}{1 - \Psi_{j,j-1}R_{j,j+1}} \exp(2ik_{j-1,z}h_{j-1}) , \quad (133)$$

$$R_{N,N+1} = 0$$

$$\Psi_{j-1,j} = \frac{k_{j-1,z} - k_{j,z}}{k_{j-1,z} + k_{j,z}} \exp\left(-2k_{j-1,z}k_{j,z}\sigma_{j-1,j}^{\ 2}\right), \quad \Psi_{j,j-1} = -\Psi_{j-1,j} , \quad (131)$$

$$\Phi_{j-1,j} = \frac{2k_{j-1,z}}{k_{j-1,z} + k_{j,z}} \exp\{-[C_1(k_{j-1,z} - k_{j,z})^2 + C_2 k_{j-1,z}k_{j,z}]\sigma_{0,1}^{\ 2}\},$$

$$\Phi_{j,j-1} = \Phi_{j-1,j}\frac{k_{j,z}}{k_{j-1,z}} \quad , \quad (132)$$

where parameters C_1, C_2 depend on the proposed approximation. In the present work, we choose $C_1 = 2$ and $C_2 = 0$, which, we believe, is the most appropriate approximation.

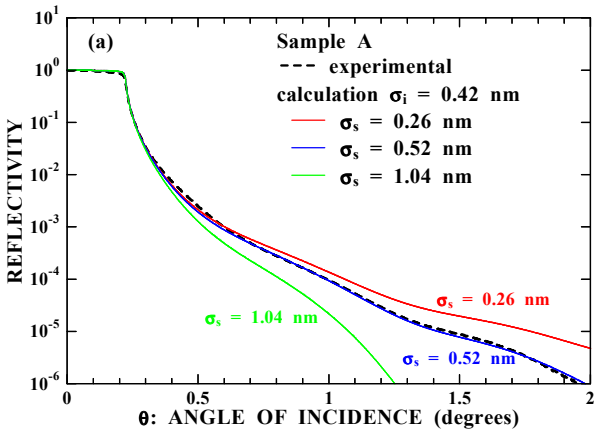

Fig. 17(a). X-ray reflectivity from the sample A. The experimental result (thick dashed curve) is compared with the calculated ones for σi = 0.42 nm and various σs (thin curves).

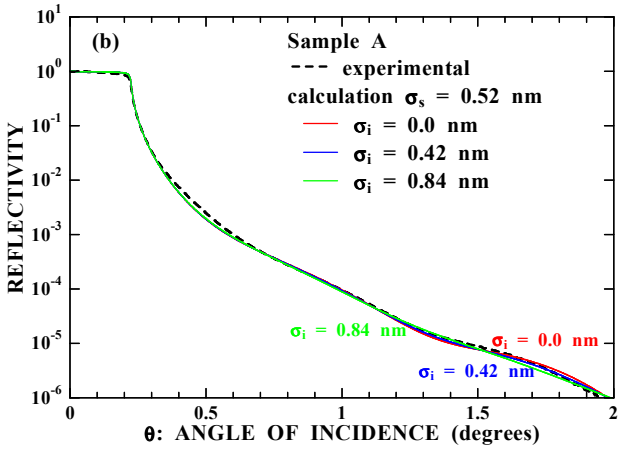

Fig. 17(b). X-ray reflectivity from the sample A. The experimental result (thick dashed curve) is compared with the calculated ones for σ_s = 0.52 nm and various σ_i (thin curves).

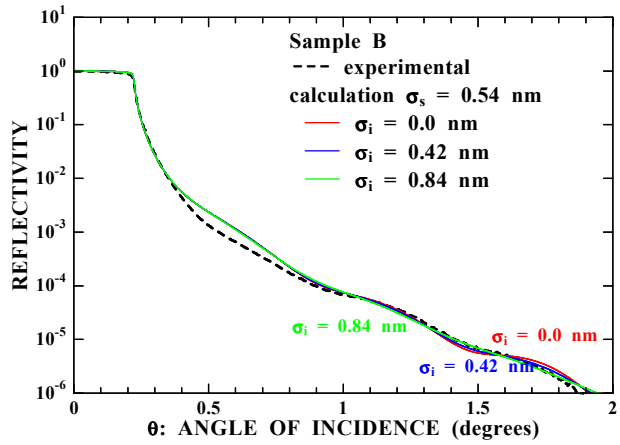

Fig. 18(a). X-ray reflectivity from the sample B. The experimental result (thick dashed curve) is compared with the calculated ones for σ_s = 0.54 nm and various σ_i (thin curves).

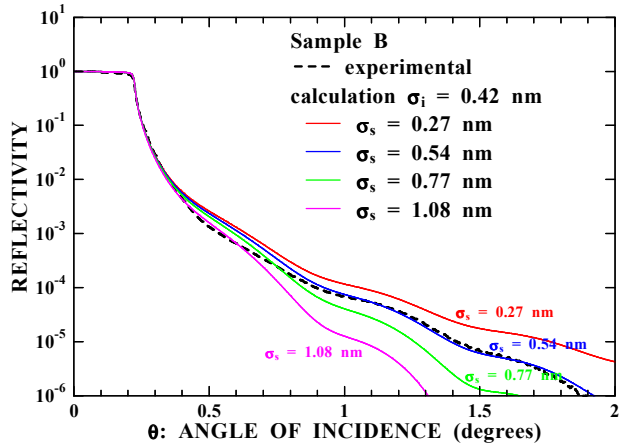

Fig. 18(b). X-ray reflectivity from the sample B. The experimental result (thick dashed curve) is compared with the calculated ones for σi = 0.42 nm and various σs (thin curves).

As was mentioned above, the origin of the oscillation is the interference between the x-rays reflected from the surface and the interface. Thus the thickness of the SiO_2 layer can be determined from the observed period of the oscillation. The

detailed procedure to derive the layer thickness from the observed period of the oscillation can be found in literatures [1]. The obtained thickness of SiO_2 of sample A is 5.3 nm, which is in good agreement with the HRBS result (5.2 nm).

Using Eqs. (131) – (133) and the above determined thickness of SiO_2 (5.3 nm), the reflectivity was calculated with various values of σ_s and σ_i, where the sample was treated as three layers (vacuum/SiO_2/Si). The calculated results are compared with the experimental one in Figs. 17a and 17b. It is seen that the overall θ_i–dependence of the reflectivity is sensitive to σ_s (see Fig. 17a, where the results for [σ_s, σ_i] = [0.26 nm, 0.42 nm], [0.52 nm, 0.42 nm], [1.04 nm, 0.42 nm] are shown). When σ_s is increased the calculated reflectivity decreases more rapidly with θ_i. This indicates that the surface roughness can be accurately determined by comparing the θ_i–dependence of the calculated results with the experimental one. The best fit was obtained when the surface roughness is 0.52 nm in the present case.

On the other hand, accurate determination of σ_i is rather difficult by XRR because the calculated θ_i–dependence of the reflectivity hardly depends on σ_i (see Fig. 17b, where the results for [σ_s, σ_i] = [0.52 nm, 0 nm], [0.52 nm, 0.42 nm], [0.52 nm, 0.84 nm] are shown). In order to estimate σ_i, the result of HRBS (σ_t = 0. 67 nm) can be used. Assuming that there is no correlation between the surface and interface roughnesses, the interface roughness σ_i can be given by $(\sigma_t^2 - \sigma_s^2)^{1/2}$ = 0.42 nm. The calculated reflectivity for σ_s = 0.52 nm, σ_i = 0.42 nm is shown by a solid line in Figs. 17a and 17b. The agreement with the experimental result is reasonably good.

A similar procedure was applied to analyse the XRR data of sample B. From the period of the oscillation, the thickness of the SiO_2 layer was determined to be 7.8 nm, which is again in good agreement with the HRBS result (7.4 nm). Using Eqs. (131) – (133), the reflectivity was calculated with various values of σ_s and σ_i. Some examples of the calculated results are compared with the experimental one in Fig. 18a. Similarly to the sample A, the calculated reflectivity hardly changes with σ_i and the determination of σ_i is difficult. Because the deposition of the additional SiO_2 layer of 2 nm does not change the interface roughness we used the interface roughness determined for the sample A (σ_i = 0.42 nm) in the estimation of the surface roughness of the sample B. Using these values (σ_i = 0.42 nm and the thickness 7.8 nm) the reflectivity was calculated with various values of σ_s. Figure 18b shows the comparison between the calculated and experimental results. Differently from the sample A, none of the calculated results can reproduce the experimental one. At $\theta_i > 1.0°$ the calculated result for σ_s = 0.54 nm agrees with the experimental one while the calculated result deviates from the experimental one at smaller θ_i. On the other hand, the calculated result for σ_s = 1.08 nm agrees with the experimental one at smaller θ_i but it deviates seriously with increasing θ_i. A possible explanation of the present discrepancy may be that the effective surface roughness measured by XRR depends on the size of the effective probing area on the surface, which is proportional to $1/\sin\theta_i$. In general, the surface roughness increases with increasing size of the probing area. As a result, the effective roughness observed at smaller θ_i is larger than that at larger θ_i in accordance with the present result. Such a θ_i-dependence of the effective roughness in XRR has been usually neglected. The present result, however, indicates that it should be taken into account in the cases like the sample B, of which the effective roughness depends on the size of the probing area. In passing we note that the probing area of the present HRBS measurement was 3.5 × 2 mm^2. The surface roughness of sample B in this probing area can be estimated to be 0.77 nm (= $[\sigma_t^2 - \sigma_i^2]^{1/2}$) using σ_t = 0.88 nm, which was determined by HRBS, and the interface roughness σ_i = 0.42 nm. The calculated reflectivity with thus determined σ_s = 0.77 nm agrees with the observed XRR result around θ_i = 0.8° (see Fig. 18b), where the probing area is 3.6 (= 0.05/sin(0.8°)) × 2 mm^2. This indicates that both HRBS and XRR give the same surface roughness if the probing areas are same.

The present result shows that the surface roughness of the sample B depends on the size of the probing area while the sample A does not. The difference between the samples may be ascribed to the difference in the preparation method. The sample A was prepared by thermal oxidizing of a Si(001) wafer, which generally results in a very flat surface. The sample B, on the other hand, was prepared by vacuum deposition of an additional SiO_2 layer on the sample A.

From AFM observations, the surface roughness σ_s of the SiO_2 surfaces of sample A and sample B were showed as 0.17 nm at the area of 1 × 1 μm^2 and 0.24 nm at the area of 10 × 10 μm^2. Both of these results are different with the XRR results. The surface roughness estimated from AFM observation show small value with those of x-ray reflectivity and smaller at the area of 1 × 1 μm^2 than at the area of 10 × 10 μm^2. This suggests that the value of roughness measured by the measurement range may be different in the x-ray reflectivity measurements. And in the x-ray reflectivity measurement, the measurement range changes by an incidence angle, and changes very much at small glancing incidence angle. This suggests that size of the different roughness depending on an incidence angle in a calculation of the x-rays reflectivity should be assume. This is the new thought that nobody considered in x-ray reflectivity calculation previously.

5. Analysis of Surface Roughness Correlation Function by X-ray Reflectivity

In this section, we show the improved formulae of XRR which derives more accurate surface and interface roughness with depending on the size of coherent X-rays probing area.

We show again the Fresnel coefficient $\Psi_{j-1,\,j}$ for reflection and the Fresnel coefficient $\Phi_{j-1,\,j}$ for refraction as,

$$\Psi_{j-1,j} = \frac{k_{j-1,z} - k_{j,z}}{k_{j-1,z} + k_{j,z}} Q_{j-1,j}, \quad \Psi_{j,j-1} = -\Psi_{j-1,j}, \tag{134}$$

$$\Phi_{j-1,j} = \frac{2k_{j\text{-}1,z}}{k_{j\text{-}1,z} + k_{j,z}} P_{j-1,j}, \quad \Phi_{j,j-1} = \Phi_{j-1,j} \frac{k_{j,z}}{k_{j\text{-}1,z}}, \tag{135}$$

where $Q_{j\text{-}1,\,j}$ and $P_{j\text{-}1,\,j}$ are the reduce factor due to the roughness, and used the following approximations formula as,

$$Q_{j-1,j} = \exp\left(-2k_{j-1,z}k_{j,z}\sigma_{j-1,j}{}^2\right) \tag{136}$$

$$P_{j-1,j} = \exp\{-[C_1(k_{j-1,z} - k_{j,z})^2 + C_2 k_{j-1,z}k_{j,z}]\sigma_{j-1,j}{}^2\}, \tag{137}$$

where parameters C_1, C_2 depend on the proposed approximation as above.

Now we consider about the reduce factor due to the roughness again. Previous work [17-23], X-ray scattering from rough surface is studied, and the effect of the roughness is explained as,

$$Q_{j-1,j} = \frac{\iint_{S_0} e^{-k_{j-1,z}k_{j,z}g(x,y)} e^{-i(q_x x + q_y y)} dxdy}{\iint_{S_0} e^{-i(q_x x + q_y y)} dxdy}, \; q_x = k_{j,x} - k_{j,x} \;,\; q_y = k_{j,y} - k_{j,y} \tag{138}$$

$$P_{j-1,j} = \frac{\iint_{S_0} e^{-1/4(k_{j-1,z} - k_{j,z})^2 g(x,y)} e^{-i(q_x x + q_y y)} dxdy}{\iint_{S_0} e^{-i(q_x x + q_y y)} dxdy}, \; q_x = k_{j-1,x} - k_{j,x} \;,\; q_y = k_{j-1,y} - k_{j,y}, \tag{139}$$

where $\boldsymbol{g}(\boldsymbol{x},\boldsymbol{y}) = \left\langle \{z(\boldsymbol{x}'+\boldsymbol{x},\boldsymbol{y}'+\boldsymbol{y}) - z(\boldsymbol{x}',\boldsymbol{y}')\}^2 \right\rangle$ is the square average of the height of the interface at (x'+x,y'+y) separated by (x,y) from (x',y').In the reflected X-ray and the refracted X-ray, qx=qy=0.The scattering plane, x-z plane, is considered in the analysis on X-ray reflectivity. Then the reduce factor Qj-1, j and Pj-1, j are shown as,

$$Q_{j-1,j} = \frac{1}{L_x} \int_{L_x} e^{-k_{j-1,z}k_{j,z}g(x)} dx, \tag{140}$$

$$P_{j-1,j} = \frac{1}{L_x} \int_{L_x} e^{-1/4(k_{j-1,z} - k_{j,z})^2 g(x)} dx, \tag{141}$$

where l_x is the length of the probing area of coherent X-ray. The square average $g(x)$ of the height of the interfaceis related to the roughness correlation function $C(x)$ as,

$$g(x) = 2\sigma^2 - 2C(x) \tag{142}$$

Following Shinha et al. (Sinha et al., 1988), the roughness correlation function $C(x)$ of a fractal surface has the form as,

$$g(x) = 2\sigma^2 \left[1 - \exp\left\{-\left(\frac{|x|}{\xi}\right)^{2H}\right\}\right], \tag{143}$$

where Hurst parameter H $(0 < H \le 1)$ is connected to its fractal dimension, and the lateral correlation length ξ acts as a cutoff length for the fractal behavior of the surface.

Then the reduce factor shows as the following;

$$Q_{j-1,j} = \int_0^1 \exp\left(-2k_{j-1,z}k_{j,z}\sigma_{j-1,j}{}^2\left[1 - \exp\left\{-\left(\frac{L_x x}{\xi_{j-1,j}}\right)^{2H}\right\}\right]\right) dx,$$

$$P_{j-1,j} = \int_0^1 \exp\left(-\frac{1}{2}(k_{j-1,z} - k_{j,z})^2 \sigma_{j-1,j}{}^2\left[1 - \exp\left\{-\left(\frac{L_x x}{\xi_{j-1,j}}\right)^{2H}\right\}\right]\right) dx, \tag{144}$$

when $\xi << L_x$, $g(x)$ becomes $2\sigma^2$, and the reduce factor $Q_{j\text{-}1,j}$ becomes Eq.(136). Now we assumed that the roughness include the part without lateral correlation, i.e., σ' when $\xi = 0$. Then the square average $g(x)$ of the height of the interface becomes;

$$g(x) = 2\sigma^2 \left[1 - \exp\left\{-\left(\frac{|x|}{\xi}\right)^{2H}\right\}\right] + 2\sigma'{}^2. \tag{145}$$

Then the reduce factor shows as the following;

$$Q_{j-1,j} = \int_0^1 \exp\left(-2k_{j-1,z}k_{j,z}\left[\sigma''_{j-1,j}{}^2 - \sigma_{j-1,j}{}^2 \exp\left\{-\left(\frac{L_x x}{\xi_{j-1,j}}\right)^{2H}\right\}\right]\right) dx, \tag{146}$$

$$P_{j-1,j} = \int_0^1 \exp\left(-\frac{1}{2}(k_{j-1,z} - k_{j,z})^2\left[\sigma''_{j-1,j}{}^2 - \sigma_{j-1,j}{}^2 \exp\left\{-\left(\frac{L_x x}{\xi_{j-1,j}}\right)^{2H}\right\}\right]\right) dx. \tag{147}$$

And we assume more approximation on integral of double exponential function that replace a value of the integral calculus with the value of the integrand at x=1. Then the reduce factor shows as the following;

$$Q_{j-1,j} = \exp\left(-2k_{j-1,z}k_{j,z}\left[\sigma''_{j-1,j}{}^2 - \sigma_{j-1,j}{}^2 \exp\left\{-\left(\frac{L_x}{\xi_{j-1,j}}\right)^{2H}\right\}\right]\right), \tag{148}$$

$$P_{j-1,j} = \exp\left(-\frac{1}{2}(k_{j-1,z} - k_{j,z})^2\left[\sigma''_{j-1,j}{}^2 - \sigma_{j-1,j}{}^2 \exp\left\{-\left(\frac{L_x}{\xi_{j-1,j}}\right)^{2H}\right\}\right]\right) \tag{149}$$

Now we show the reduce factor with using the effective roughness σ^* at the angle θ_i of incident X-ray as,

$$Q_{j-1,j} = \exp\left(-2k_{j-1,z}k_{j,z}\sigma^*_{j-1,j}{}^2\right), \tag{150}$$

$$P_{j-1,j} = \exp\left(-\frac{1}{2}(k_{j-1,z} - k_{j,z})^2 \sigma^*_{j-1,j}{}^2\right), \tag{151}$$

where the effective roughness σ^* can be defined approximately as,

$$\sigma^*{}_{j-1,j}{}^2 = \sigma''_{j-1,j}{}^2 - \sigma_{j-1,j}{}^2 \exp\left\{-\left(\frac{L_x}{\xi_{j-1,j}}\right)^{2H}\right\}, \tag{152}$$

Note that we implicitly assumed that ξ is smaller than the coherence length L_x of the radiation parallel to the surface. L_x depends on the angle θ_i of incident X-ray as,

$$\frac{1}{L_x^2} = \frac{\sin^2\theta_i}{L_t^2} + \frac{\cos^2\theta_i}{L_l^2}, \tag{153}$$

where L_t is transverse coherence length and L_l is longitudinal coherence length of the incident X ray.

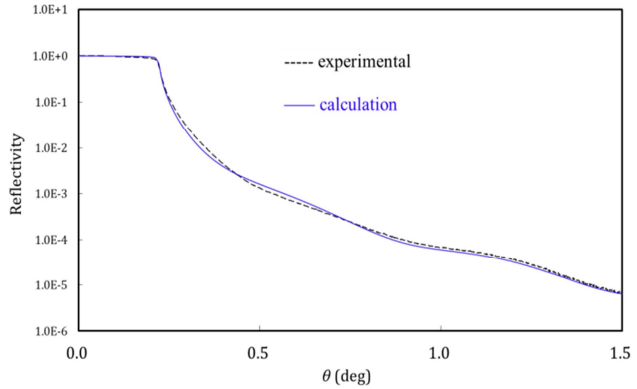

Figure 19. *X-ray reflectivity from sio₂/Si. The experimental result (thick dashed curve) is compared with the calculated ones usingthe effective roughness depending onthe X-ray incident angle θ_i. XRR is calculated with using the values (ξ_s = 2μm, L_t = 10nm, and L_l = 2μm).*

Based on the above considerations, we again calculated the X-ray reflectivity for the SiO_2/Si surface of sample B, but now consideredthe effective roughness σ * at the X-ray incident angle θ_i. Figure 2 shows the calculated XRR with using the values (ξ_s = 2μm, L_t = 10nm, and L_l= 2μm). The calculated reflectivity shows good agreement with the experimental one in all range of measured θ_i.

6. Summary

In this review, we investigated the fact that the calculated result of the x-ray reflectivity based on Parratt formalism [1] with the effect of the roughness incorporated by the theory of Nevot-Croce[2] show a strange phenomenon in which the amplitude of the oscillation due to the interference effects increase in the case of the rougher surface. The strange result had its origin in a serious mistake that the diffuse scattering at the rough interface was not taken into account in the equation. Then we developed new improved formalism to correct this mistake. The new, accurate formalism is completely described in detail. The x-ray reflectivity R of a multilayer thin film material consisting of N layers is derived by the use of accurate reflectivity equations for $R_{j-1,\,j}$ and $R_{j,j+1}$ as following,

$$\begin{aligned} &R = \left|R_{0,1}\right|^2, \\ &R_{j-1,j} = \frac{\Psi_{j-1,j} + (\Phi_{j-1,j}\Phi_{j,j-1} - \Psi_{j-1,j}\Psi_{j,j-1})R_{j,j+1}}{1 - \Psi_{j,j-1}R_{j,j+1}} \exp(2ik_{j-1,z}h_{j-1}), \\ &R_{N,N+1} = 0 \end{aligned} \tag{150}$$

Here, the refractive index of the j-th layer $n_j = 1 - \delta_j - i\beta_j$, $n_0 = 1$, the z-direction component of the wave vector of the j-th layer $k_{j,z} = k\sqrt{n_j^2 - \cos^2\theta}$, k=2π/λ, λ; wave length, θ; glancing angle of incidence, a N-layer multilayer system with a j-th layer of thickness of h_j and j-1,j-th interface roughness of $\sigma_{j\text{-}1,j}$, $k_{j,\,z}$ is the z component of the wave vector in the j-th layer, and $\Psi_{j\text{-}1,\,j}$ and $\Phi_{j\text{-}1,\,j}$ are the Fresnel coefficients for reflection and refraction, respectively, at the interface between the (j-1)th layer and the j-th layer.

$$\Psi_{j-1,j} = \frac{k_{j-1,z} - k_{j,z}}{k_{j-1,z} + k_{j,z}} Q_{j-1,j}, \quad \Psi_{j,j-1} = -\Psi_{j-1,j}, \tag{151}$$

$$\Phi_{j-1,j} = \frac{2k_{j-1,z}}{k_{j-1,z} + k_{j,z}} P_{j-1,j}, \quad \Phi_{j,j-1} = \Phi_{j-1,j}\frac{k_{j,z}}{k_{j-1,z}}, \tag{152}$$

where the reduce factor Q and P are showed with using the effective roughness σ* at the angle θ_i of incident X-ray as,

$$Q_{j-1,j} = \exp\left(-2k_{j-1,z}k_{j,z}\sigma^{*2}_{j-1,j}\right), \tag{153}$$

$$P_{j-1,j} = \exp\left(-\frac{1}{2}(k_{j-1,z} - k_{j,z})^2\sigma^{*2}_{j-1,j}\right), \tag{154}$$

where the effective roughness σ* can be defined approximately as,

$$\sigma^{*2}_{j-1,j} = \sigma''^{2}_{j-1,j} - \sigma^2_{j-1,j}\exp\left\{-\left(\frac{L_x}{\xi_{j-1,j}}\right)^{2H}\right\}, \tag{155}$$

L_x depends on the angle θ_i of incident X-ray as,

$$\frac{1}{L_x^2} = \frac{\sin^2\theta_i}{L_t^2} + \frac{\cos^2\theta_i}{L_l^2}, \tag{156}$$

where L_t is transverse coherence length and L_l is longitudinal coherence length of the incident X ray. Note that we implicitly assumed that ξ is smaller than the coherence length L_x of the radiation parallel to the surface.

The reflectivity calculated with this accurate formalism gives a physically reasonable result. The use of this equation resolves the strange numerical results that occurred in the previous calculations that neglected diffuse scattering and is expected that buried interface structure can now be analyzed more accurately.

In concerned with the calculation of XRR, we considered the effective roughness with depending on the incident angle of X-ray. At the result, it is showed the new improved XRR formalism which derives more accurate surface and interface roughness with depending on the size of coherent X-rays probing area, and derives the roughness correlation function and the lateral correlation length.

References

[1] Parratt L. G., *Phys. Rev.* 95, 359-369 (1954).

[2] Nevot L. and Croce P., *Rev. Phys. Appl.* 15 761-779 (1980).

[3] Yoneda Y., Phys. Rev. 131, 2010 (1963).

[4] Marra W. C., Eisenberger P., and Cho A. Y., *J. Appl. Phys.* 50 6927 (1979).

[5] Vineyard G. H., *Phys. Rev.* B 50, 4146 (1982).

[6] Robinson I. K., *Phys. Rev.* B 33 3830 (1986).

[7] Sakurai K., and Iida A., *Jpn. J. Appl. Phys.* 31, L113 (1992).

[8] Sakaida Y., Harada S., and Tanaka K., *J. Soc. Mat. Sci. Japan* 42-477, 641 (1993).

[9] Fujii Y., Nakayama T., and Yoshida K., *ISIJ International* 44 1549-1553 (2004).

[10] Fujii Y., Komai T., and Ikeda K.; *Surf.Interface Anal.* 37, 190-193 (2005).

[11] Fujii Y., Yanase E., and Arai K., *Applied Auface Science* 244, 230 (2005).

[12] Fujii Y., and Nakayama T., *Surf. Interface Anal.* 38, 1679 (2006).

[13] Fujii Y., Yanase E., and Nishio K., *J. Phys.: Conf. Ser.*, 83, 012008 (2007).

[14] Fujii Y., *Surf. Interface Anal.* 40, 1722 (2008).

[15] Holy V., Pietsch U., and Baumbach T., (Eds.) *High-Resolution X-Ray Scattering from Thin Films and Multilayers,* Springer, Berlin (1999).

[16] Daillant J., and Gibaud A., (Eds.) X-ray and Neutron Reflectivity, Principles and Applications, Springer, Berlin (1999).

[17] Shinha S. K., Sirota E. B., Garoff S., and Stanley H.B., *Phys. Rev.* B 38, 2297-2311 (1988).

[18] Holy V., Kubena J., Ohlidal I., Lischka K., and Plotz W., *Phys. Rev.* B 47 15896-15903 (1993).

[19] Slater C., and Frank N. H., (Eds.) *Electromagnetism*, McGraw-Hill, New York (1947).

[20] Vidal B., and Vincent P., *Applied Optics* 23 1794-1801 (1984).

[21] Boer D. K. G., Phys. Rev. B 49, 5817 (1994).

[22] Boer D. K. G., *Phys. Rev.* B 51 5297-5305 (1995).

[23] Boer D. K. G., and A. J. G. Leenaers, Physica B 221, 18 (1996).

[24] N. Awaji, and S. Komiya, J. Vac. Sci. Tecnol. A 14, 971 (1996).

[25] M. K. Sanyal, J. k. Basu, A. Datta, and S. Banerjee, Europhys. Lett. 36, 265 (1996).

[26] M. K. Sanyal, S. Hazra, J. k. Basu, and A. Datta, Phys. Rev. B 58, R4258 (1998).

[27] T. Hirano, K. Usami, and K. Ueda, Synchrotoron Rad. 5, 969 (1998).

[28] M. Tolan, X-ray Scattering from Soft-Matter Thin Films (Springer, Berlin, 1999).

[29] K. Stoev, and K. Sakurai, Spectrochim. Acta B 54, 41 (1999).

[30] E. Smigiel and A. Cornet, J. Phys. D 33, 1757 (2000).

[31] K. Ueda, Trans. MRS Japan 32, 223 (2007).

[32] Sakurai K., (Ed.) *Introduction to X-ray Reflectivity,* Kodansha Scientific, Tokyo (2009).

[33] Fujii Y., *Surf. Interface Anal.* 42 1642-1645 (2010).

[34] Fujii Y., *Mater. Sci. Eng.* 24, 012008 (9pp) (2011).

[35] Fujii Y., *Mater. Sci. Eng.* 24, 012009 (21pp) (2011).

[36] Fujii, Y., Powder Diffraction 28 (2), 100-104 (2013).

[37] Fujii, Y., Adv. Anal. Chem. 3(2), 9-14 (2013).

[38] Fujii, Y., Japanese Journal of Applied Physics. 53, 05FH06 (2014).

[39] Fujii, Y., Nakajima, K., Suzuki, M., and Kimura, K. Surf. Interface Anal. 46, 1208-1211 (2014).

[40] Fujii, Y., Powder Diffraction 29 (3), 265-268 (2014).

[41] Fujii, Y., American Journal of Physics and Applications 3(2), 21-24 (2015).

[42] K. Nakajima, S. Joumori, M. Suzuki, K. Kimura, T. Osipowicz, K. L. Tok, J. Z. Zheng, A. See, B. C. Zhang, Appl. Phys. Lett. 83, 296 (2003).

[43] K. Kimura, K. Ohshima, M. Mannami, Appl. Phys. Lett. 64, 2232 (1994).

[44] K. Kimura, S. Joumori, Y. Oota, K. Nakajima, M. Suzuki, Nucl. Instrum. Meth. B220, 351 (2004).

[45] Q. Yang, D. J. O'Connor and Z. Wang, Nucl. Instrum. Meth. B61, 149 (1991).